Interferences caused by the ~~microbial~~ biogeochemical methane cycle in peats during the assessment of abandoned oil ~~and gas~~ wells

Sebastian F. A. Jordan[1]*, Stefan Schloemer[1], Martin Krüger[1], Tanja Heffner[2], Marcus A. Horn[2], Martin Blumenberg[1]*

[1]Federal Institute for Geosciences and Natural Resources (BGR), Hannover, Stilleweg 2, 30655, Germany
[2]Leibniz Universität Hannover, Institute for Microbiology, Herrenhäuser Str. 2, Hannover, 30419, Germany

Correspondence to: Sebastian F. A. Jordan (Sebastian.Jordan@bgr.de), Martin Blumenberg (Martin.Blumenberg@bgr.de)

Abstract.

In the global effort to reduce anthropogenic methane emissions, the millions of abandoned oil and gas wells are suspected to be prominent but so far often overlooked methane sources. Recent studies have highlighted the hundreds of thousands of undocumented abandoned wells in North America as ~~sometimes strong~~major methane ~~emitters~~sources, sometimes ~~with~~ emitting up to several tons of methane per year. ~~However, the majority of studies focused on abandoned wells with their surface installations still in place. Only a few studies examined cut and buried wells as their exact location are often unknown.~~ In Germany, approximately 20,000 abandoned wells ~~are~~ have been described, which are well documented, and the data is publically available. Here we present a methodological approach to assess particularly methane emissions from ~~such~~ cut and buried abandoned wells, which are typical for Germany. We sampled eight oil wells in a ~~peat~~ peat-rich ~~setting~~ environment with four wells in a forest, three wells in an active peat extraction site, and one well on a meadow. All three areas ~~have~~ are underlain by peat ~~deposits underneath~~. At each site, we sampled a 30 x 30 m grid and a corresponding 20 x 20 m reference grid. Three of the eight wells and reference sites exhibited net methane emissions. In each case, the reference sites emitted more methane than the respective well site with the highest net emission (~110 nmol CH_4 m^{-2} s^{-1}) observed at one of these reference sites.~~Three of the eight well and reference sites showed net methane emissions. The highest emissions with up to ~110 nmol CH_4 m^{-2} s^{-1} were observed at one of the reference sites.~~ All ~~three~~ methane-emitting sites were located within the active peat extraction area. Detailed soil gas characterization revealed no methane, ethane, and propane ratio typical for reservoir gas, but instead showed a typical biogenic composition and isotopic signature (mean $\delta^{13}C$-CH_4 –63‰). ~~Accordingly~~Thus, the escaping methane did not originate from the abandoned wells or the ~~connected~~ associated oil reservoir. ~~In addition~~Furthermore, isotopic signatures of methane and carbon dioxide suggest that the methane from the peat extraction site~~'s methane~~ was produced by acetoclastic methanogens, whereas the methane at the meadow site was ~~from~~ produced by hydrogenotrophic methanogens. However, our genetic analysis showed that both types of methanogens were present at both sites, suggesting that ~~and thus~~ other factors ~~were c~~control~~ling~~ the ~~prevailing~~ dominant methane production ~~mechanism~~pathway. Subsequent molecular biological ~~investigations highlighted~~studies confirmed ~~–~~that aerobic ~~methanotrophs~~ methanotrophic bacteria were also important and that the~~y had the highest~~ir relative abundance was highest at the peat extraction site.

Furthermore, the composition of the methanotrophic community varied ~~across~~ between sites and depths. The aerobic methane oxidation rates were highest at the peat extraction site potentially oxidizing a multiple of the emitted methane, thus likely providing an effective microbial methane filter.

For the assessment of potential leakage from cut and buried abandoned wells, ~~O~~our ~~findings~~ results ~~underscore the necessity~~highlight the need to combine methane emissions with ~~the~~ soil gas characterization ~~of soil gases~~ in comparison ~~with~~ to a suitable reference site. A monitoring that relies exclusively on methane emissions may result in erroneous classification of naturally occurring emissions as well integrity failure~~to survey cut and buried abandoned wells as a solely emission based surveillance could misinterpret natural occurring emissions~~.

1 Introduction

Methane is one of the key greenhouse gases contributing to climate change. It has, however, a particular role in climate change mitigation, too, as its atmospheric lifetime is especially short (Saunois et al., 2020). This makes methane the prominent political target, because emission reduction may quickly result in decreasing atmospheric concentration and, thus, climate effect. In total 156 countries participate in the global methane pledge aiming to reduce global methane emissions by 30% until 2030 (IEA, 2024).

The fossil fuel sector is the second largest anthropogenic methane source. Methane emissions from this sector not only include emissions from active production but also leakage from millions of abandoned oil and gas wells, due to well integrity failure as recent studies found, e.g., in the USA and Canada (Samano et al. 2022, Williams et al. 2021). The permanently increasing number ~~slow decay~~ of global abandoned oil and gas infrastructure is a rising problem (Bowman et al. 2023, Williams et al. 2021, Riddick et al. 2020), which will intensify in the future during the transition to renewable energy sources. Abandonment procedures today depend on national regulations and are now often similar although they have differed strongly in the past. However, the greatest impact on the country's abandoned well situation has probably been the extent to which these regulations were properly enforced. Some countries are additionally struggling with the situation of undocumented or orphaned wells (Boutot et al. 2022). ~~Depending on the country's regulations, abandonment~~ Different well abandonment practices throughout history have meant that in some cases only the well head has been closed and everything has been left in place while the well casing was unplugged (Pekney et al. 2018, Williams et al. 2020), in others an open bore hole was left in the ground (Pekney et al. 2018, Lebel et al. 2020), or the wells were properly plugged, cut and the remains buried ~~could mean to just close the well head but leave everything in place (Pekney et al. 2020, Williams et al. 2020), decommission the well and leave an open hole in the ground (Pekney et al. 2020, Lebel et al. 2020), or properly fill the well and cut and burry the remains~~ (Davies et al. 2014, Schout et al. 2019~~, Davies et al. 2014~~, Cahill et al. 2023). ~~This resulted in varying situations around the world and a general call to action as anthropogenic methane emissions need to be cut (Saunois et al., 2020).~~ Thus, authorities and scientists ~~rush~~ try to identify ~~super and mega~~particular high emitters (Bowman et al 2023) or wells with a high risk of integrity failure (Cahill

and Samano 2022) to maximize economic and environmental benefits (Kang et al. 2021) as financial resources for proper well decommission are limited (Raimi et al. 2021, Agerton et al. 2023). In Germany for example, first regulations date back to 1904 and were refined every few decades to the last update of 2006 (von Georne et al. 2010). All kinds of wells (exploration, production, appraisal and injection wells) are generally decommissioned and buried (Landesamt für Bergbau, Energie und Geologie (LBEG), 1998).

It is therefore not possible to detect methane emissions from such wells using the same methods as for wells with visible surface installations, such which are partly found in the US and Canada (Williams et al. 2021, Lebel et al. 2020). For cut and buried wells (e.g., in Germany, the Netherlands, and UK), single measurements atop the wells location are insufficient (Schout et al. 2019). ~~However, this straightforward methodology is only applicable for abandoned wells with visible remains at the surface. In countries with regulations to cut and burry wells (e.g., Germany, the Netherlands, and UK), single measurements at the wells location are insufficient (Schout et al. 2019~~In this case, upwards migrating natural gas can be subject to several physical and biogeochemical processes, e.g., microbial oxidation is able to alter concentrations and even isotopic composition (Whiticar 2020). Leaking gas can even migrate away from the wells location (Dennis et al 2022, Forde et al. 2019a), disperse through the soil and potentially be oxidized by methanotrophic microorganisms on its way to the atmosphere (Forde et al. 2022). Thus, false negative results on the well integrity would be obtained. In addition, biogenic methane can be microbially produced in shallow anoxic soils by methanogenesis. Thereby, organic carbon degradation facilitated via a complex network of trophically linked microorganisms (e.g., intermediary ecosystem metabolism, Drake et al. 2009) ultimately resulting in methane production when alternative electron acceptors except for carbon dioxide are depleted (Whiticar 2020). Methanogenesis is mainly carried out by three types of anaerobic archaea in more than 30 genera: 1) acetoclastic methanogens converting acetate to methane and carbon dioxide, 2) hydrogenotrophic methanogens, reducing carbon dioxide to methane with hydrogen, and 3) methylotrophic methanogens disproportionating methyl groups to methane and carbon dioxide (Liu and Whitman, 2008). Although most methanogenic species are hydrogenotrophs, two-thirds of biologically produced methane is derived from acetate (Liu and Whitman, 2008). ~~). Even with correct coordinates, emissions can migrate away from the wells location (Dennis et al 2022, Forde et al. 2022), disperse through the soil and potentially be oxidized by methanotrophic microorganisms on its way to the atmosphere (Forde et al. 2022).~~Combining isotopic composition of methane and the relation of methane to the sum of ethane and propane is an often-used method to distinguish natural gas (commonly thermogenic) from biogenic methane (Whiticar 2020). However, methane can further be oxidized by anaerobic and aerobic methanotrophs to carbon dioxide along its way to the atmosphere, which shifts the isotopic composition, adding more complexity. In case of organic rich soils or soils with a high groundwater table, methane production can outweigh its consumption leading to substantial methane emissions (Le Mer and Roger 2001, Lai 2009). To put this into perspective, upland forests are known to act as methane sink taking up to ~–4 nmol m^{-2} s^{-1} methane from the atmosphere, whereas natural wetlands emit up to ~600 nmol CH_4 m^{-2} s^{-1}, which can be topped by rice paddy fields with over 2000 nmol CH_4 m^{-2} s^{-1} (Oertel et al. 2016). In general, these processes are taking place in the active zone of the soil in general but especially environments with biogenic methane

generation are prone to generate false positive well leakage classification ~~In natural methane rich environments, however biogenic methane emissions could be mistaken for a leaking well~~.

~~-~~An example for such ~~an~~ complex environments are wetlands and peat rich areas that are associated with ~~a large number of oil and gas wells in Germany.~~ ~~In Germany ~~~ 2700 abandoned wells in Germany (mainly in Northern Germany), ~~which~~ translateings to roughly 15% of all abandoned German wells (~~20~~4,000; NIBIS® Kartenserver 2014b, Wittnebel et. al., 2023)~~) are situated in an organic rich soil (mainly peats) setting (Wittnebel et al., 2023)~~. Thus, these areas act as an ideal test ground for method testing.

Peat rich areas are biogeochemical complex and are defined as former raised/ombrotrophic bogs, rich fens and other types of peat accumulating wetlands. In the pristine ecosystems, the vegetation is taking up carbon dioxide from the atmosphere and producing biomass.~~, the vegetation is taking up carbon dioxide from the atmosphere and producing biomass.~~ Peat accumulates as ~~Plant~~ plant litter and is only partially decomposed due to oxygen limitation (Turetsky et al., 2014; Frolking et al., 2006) below the partially aerated and very thin vadose zone~~in deeper layers~~. ~~Once oxygen is depleted the microbial degradation of organic carbon is coupled to the reduction of a series of terminal electron acceptors depending on their half cell potentials (Sikora et al., 2017). Organic carbon degradation is facilitated by a complex network of trophically linked microorganisms (i.e., intermediary ecosystem metabolism) ultimately resulting in methane production when alternative electron acceptors except for carbon dioxide are depleted (Whiticar 2020). Methanogenesis is mainly carried out by three types of anaerobic archaea in more than 30 genera: 1) acetoclastic methanogens converting acetate to methane and carbon dioxide, 2) hydrogenotrophic methanogens, reducing carbon dioxide to methane with hydrogen, and 3) methylotrophic methanogens disproportionating methyl groups to methane and carbon dioxide (Liu and Whitman, 2008). Although most methanogens are hydrogenotrophs, two thirds of biologically produced methane is derived from acetate (Liu and Whitman, 2008). Is sufficient methane produced, it diffuses towards the surface and it is partially oxidized by anaerobic and aerobic methanotrophs to carbon dioxide along the way. Methanotrophs thereby act as an efficient methane filter and are associated with the regulation of methane fluxes from wetlands. However, these wetlands are still active net carbon sinks, since CO_2 fixation in plant biomass by far exceeds biomass mineralization, and accumulate peat for millennials ~~(Turetsky et al., 2014; Frolking et al., 2006)~~. ~~Thus, wetlands play a relevant role in the global C cycle as important terrestrial carbon pool (Belyea, 2013).~~

However, ~~M~~most raised bogs in Central Europe were~~, however,~~ drained in the past for agricultural use, forest cultivation, and peat extraction for fuel or horticultural purposes (Pfadenhauer and Klötzli, 1996; Laine et al., 2013). After drainage, most of these wetlands change from net carbon sinks to net carbon sources (Frolking et al., 2006). This is due to the remineralization of once stored organic matter to ultimately carbon dioxide (Abdalla et al., 2016). ~~On the other hand~~Then again, methane emission decreases drastically as the aerated soils enable aerobic methane oxidation to CO_2 and methanogenesis is restricted to deeper layers (Sundh et al., 1994; Abdalla et al., 2016). Nonetheless, the greenhouse gas balance changes with drainage and differs depending on land use (Abdalla et al., 2016). Methane emissions are thought to stop altogether in peatlands used for forestry or agriculture (Abdalla et al., 2016 and references therein). However, previous studies point towards substantial methane emissions from ditches, which are draining the peats and can even reach the magnitude of emissions from virgin

peatlands (Sundh et al., 2000). The extraction of peat results in an accelerated carbon loss and increased greenhouse gas emissions as peat decomposition associated with end use comprises the majority of total emissions (e.g., combustion and use in horticulture~~), machinery for extraction and transportation add additional emissions~~s; ~~(~~Cleary et al., 2005). In this complexity of methane ~~und~~ and carbon dioxide related biogeochemical processes in soils in general, one has to look closely to delicately allocate methane emission to natural or anthropogenic (e.g., abandoned wells) sources.

Worldwide only very few countries, ~~i.e.~~e.g., the USA and Canada (Bowman et al., 2023) include emission from abandoned wells in their yearly greenhouse gas inventory. In a BGR project "leakage assessment of buried wells in Germany", we aim to fill this knowledge gap for Germany by studying a representative sub-set of abandoned wells ~~over the course of five years~~. We use the term "abandoned well" here to refer to a former oil or gas well in Germany that has been decommissioned and buried in accordance with the guidelines in force at the time (von Georne et al. 2010). This includes plugging and backfilling of the well, cutting, and removing of the shallow casings, and reconditioning of the area (e.g. for agricultural use).

Here, we present a first detailed study of eight wells in a complex methane rich setting in Northern Germany. ~~In Germany ~ 2700 abandoned wells, which translates to roughly 15% of all abandoned wells (~20,000; NIBIS® Kartenserver 2014) are situated in an organic rich soil (mainly peats) setting (Wittnebel et al., 2023). Such soils are highly likely to produce and emit methane.~~ Environments with high in-situ biogenic methane generation might lead to a false positive well leakage classification based on surface emission measurements, if the methane source (shallow biogenic vs thermogenic natural gas) is not correctly determined. We present our ~~We used this opportunity to test our~~ principal methodological approach, a combination of geochemical and microbial techniques, to evaluate methane emissions from cut and buried abandoned wells. ~~Our main focus~~In this paper, we focus on the results from this small study area, including overall methane emissions and identifying ~~was on the question of whether we could clearly identify~~ the source of the methane, and thus allocate the emissions to the abandoned wells or in-situ methanogenic processes. In addition, the microbiological methods enabled us to quantify the methane oxidation potential of the soil, i.e., the methanotrophic methane filter function, and identify key organisms feeding on the soil methane.

2 Methods

2.1 Study site

The sampling and field measurements were conducted in March and April 2022 near Steimbke (Lower Saxony, Northern Germany), an area with ongoing and historical industrial peat production. Additional samples were taken in April 2023 from the peat extraction site and November 2023 from reference sites. Three oil fields were located around Steimbke. From these three, we focused on field Steimbke-Nord. Data including location, depth, date of drilling, etc. of wells related to this oil field as well as the other ~20,000 wells in Germany (abandoned, producing, and exploration) and data on the oil and gas fields are publicly available via NIBIS map server (NIBIS® Kartenserver 2014a, 2014b). We used this database to locate about 200 wells in the vicinity of Steimbke-Nord including 159 abandoned production wells. The oil-bearing geological horizons were

located in the Malm and Dogger (both Jurassic) in 500 ~~and~~ to 700 m depth covering an area of about 1.5 km^2. The wells were drilled between 1942 and 1950 and are typically 570 to 695 m deep. In total 3 x 10^8 t oil (and 2.9 x 10^9 m^3 oil associated natural gas) were produced until 1964 (https://nibis.lbeg.de/cardomap3/?permalink=WeOGYg3, accessed 03.05.2024). We studied and sampled eight abandoned wells, each with respective reference measurements (Figure 1, Table 1). To investigate methane emissions related to abandoned onshore wells eight cut und buried wells in the south-eastern part of this oil field covering an area of ~ 0.2 km² (Figure 1) were targeted. The eight wells are situated in three different land use types. Three wells (R-WA 272, R-WA 254, R-WA 264) are located in the western part of the area where active peat mining is ongoing with the bare peat directly at the surface (from here on "Peat" sites). Before the peat extraction in the active area began, the Peat site was also an agricultural meadow that was probably temporarily grazed and regularly fertilized with manure like the meadow at well site R-WA 275, ~ 350 m to the east (from here on "Meadow" site). Two of the four wells from the forest area (dominated by birch trees and pines) are located between the active Peat site and the Meadow (R-WA 273, R-WA 274), the remaining two in a larger forested area ~ 225 m to the north and northeast, respectively (from here on "Forest" sites). ~~These well sites can be grouped into three area types. Three out of eight wells (R-WA 254, R-WA 264, R-WA 272) lie in an active peat extraction site (from here on "Peat" sites), four (R-WA 209, R-WA 211, R-WA 273, R-WA 274) in a woodland area (from here on "Forest"), and one (R-WA 275) on a meadow (from here on "Meadow" site).~~ In case of the Forest and Meadow sites, the top soil above the peat layer was sampled, whereas at the Peat sites the peat was sampled directly. Regarding pH of the Peat site, Welpelo et al. (2024) published a pH of ~ 3.5 for a nearby rewetted part of the peat extraction area, about 2.5 km away as well as additional physicochemical parameters. Residues from the drilling and/or production were only human eye visible in the forest area. Here, cement residues likely from the rig cellar or associated infrastructure, sand from the backfill procedure, and small depressions were signs of former activity. No residues of the former well itself, like wellheads, old horsehead pumps, or any kind of piping were visible. All sample sites are situated in a peat rich area and the majority of sites include about 1.0 m or more raised-bog peat either below the topsoil (Forest, Meadow) or as bare peat at the Peat site (https://nibis.lbeg.de/cardomap3/?permalink=1baQ8yzX, accessed 03.05.2024). Peat depth in this area was taken from a geological exploration in 1983. An exemplary soil profile is shown in Fig. ~~,~~ 2d, this profile was drilled near our peat reference site (~~~~50 m west). These profiles show a peat thickness of ~1.9 m up to ~2.6 m for the peat sites with about 1 m and more already extracted since ~~2019~~2017. For sites R-WA 273, R-WA 274, R-WA 275 the state agency (https://nibis.lbeg.de/cardomap3/?permalink=1uIMU2yt, accessed 03.05.2024) estimated a peat thickness of more than 2 m~~,~~. ~~however~~However, for sites R-WA 211 and R-WA 209 peat was confirmed with more than 30 cm depth but its entire thickness is unknown.

Table 1: Overview of surveyed well locations and selected meta data. All wells were used for oil production in the past. *peat is present in all areas (Peat = active peat extraction site)

name	short name	north	east	drilling completed	depth (m)	area*
Rodewald-~~WA-~~WA 211	R-WA 211	5836503	32525924	26.10.1942	635.5	Forest

Rodewald-~~WA-~~WA 209	R-WA 209	5836399	32526148	27.08.1942	570.5	Forest
Rodewald-~~WA-~~WA 273	R-WA 273	5836338	32525761	03.08.1950	682.7	Forest
Rodewald-~~WA-~~WA 274	R-WA 274	5836299	32525835	04.07.1950	680	Forest
Rodewald-~~WA-~~WA 275	R-WA 275	5836302	32525931	21.07.1950	670	Meadow
Rodewald-~~WA-~~WA 272	R-WA 272	5836374	32525686	15.06.1950	700	Peat
Rodewald-~~WA-~~WA 254	R-WA 254	5836366	32525498	15.12.1948	695	Peat
Rodewald-~~WA-~~WA 264	R-WA 264	5836323	32525566	03.06.1950	660	Peat

Figure 1: Overview of the study site in Steimbke with the well sites and reference site measuring grids each with 17 and 9 measuring points, respectively. Abandoned wells are depicted in white dots and those studied here are named (e.g., R-WA 211 etc.). The orange dotted line outlines the rough dimensions of the oil field Steimbke-Nord. Coordinates are stated in UTM-32U (WGS84) with easting and northing planar coordinates in meter. Blue indicates the well site emission (CH_4 and CO_2) measuring grid whereas orange indicates the reference site emission (CH_4 and CO_2) measuring grids with the positions for soil gas sampling marked as white or black "x", respectively. The left inlet depicts a transect with ~1 m distance between the measuring points to assess spatial variations in an area without a well. Additional soil gas sampling points are depicted as orange circles and are shown in part in a white box for better visibility. The areas compared in this study ("Peat", "Forest", "Meadow") are also marked. The map was created using QGIS (v.3.22.3) and © Google Earth satellite images from 2015 as background.

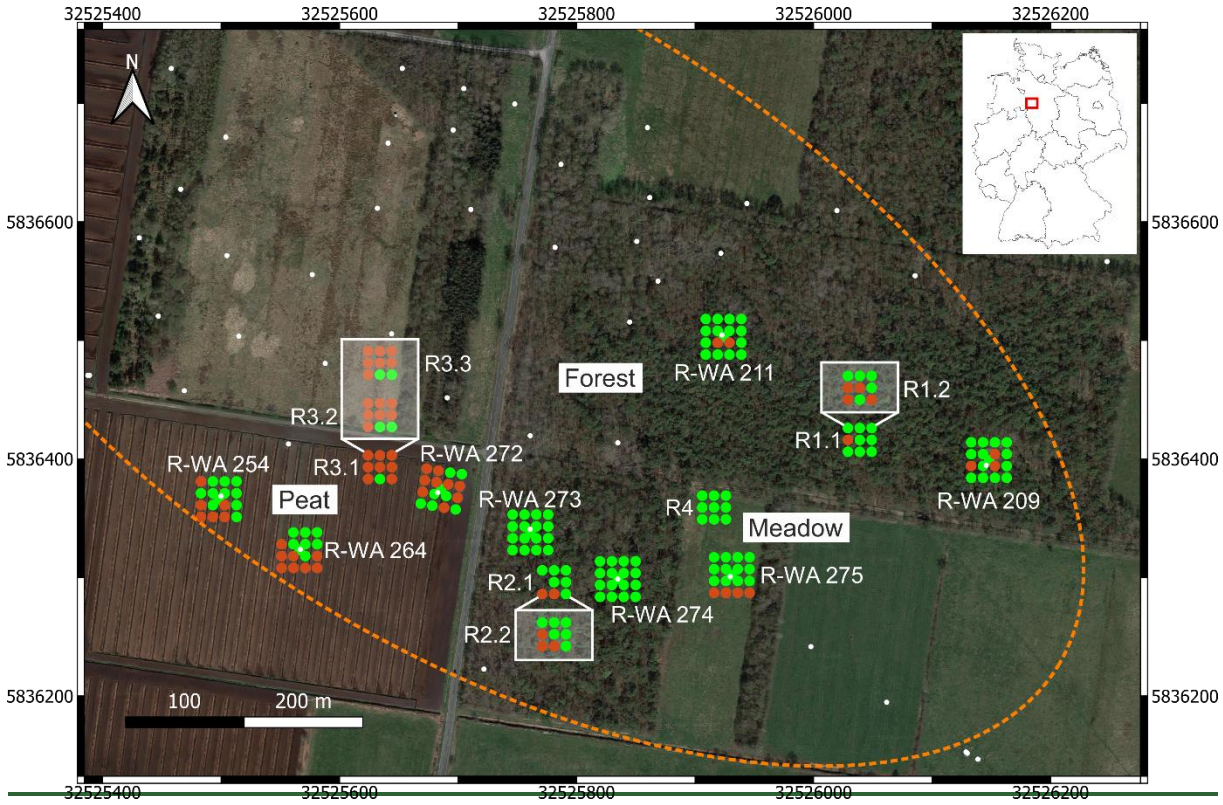

Figure 1: Overview of the study site in Steimbke with the well sites and reference site measuring grids each with 17 and 9 measuring points, respectively. Abandoned wells are depicted in white dots. The rough dimensions of the oilfield Steimbke Nord are outlined by the yellow dotted line. Coordinates are stated in UTM 32U (WGS84) with easting and northing planar coordinates in meter. Green indicates negative methane emission (methane sink) whereas red indicates positive methane emission (methane source) for each flux measuring point. The multiple measurements of reference sites are shown in a white box. The map was created using QGIS (v.3.22.3) and © Google Earth satellite images from 2015 as background.

2.2 Sampling method and grid

We studied well and reference sites for methane (and CO_2) emission (positive and negative), soil gas composition and microbial communitycommunities analysis (Figure 2c). The reference sites were placed in a distance of 15–100–150 m to any studied well on the same terrain. The position of the wells was extracted from the NIBIS® MAPSERVER (NIBIS® Kartenserver 2014), and a handheld GPS device (Garmin, etrex Vista Hcx) was used to navigate in the field. Due to the burial of abandoned wells in the working area, our study relied on the coordinates of the wells. Discussion with the LBEG, the local public as well as indications (e.g., color changes, remnants of roads/pathways) from recent and historical Google Maps images supported the correctness of the well positions.

The central measuring point was placed directly above the well. We positioned the other 16 measuring points around the well pointing north with the help of two measuring tapes and a compass. The distance between these 16 points was 10 m from point

to point aiming at a broad coverage of potential methane emission areas above the buried wells. In total, the well site grid covered an area of 30 x 30 m and 17 measuring points (Figure 2a). Soil gas samples were taken in the central five positions of the well as indicated in Fig. 2a. Soil samples for microbial analyses were usually taken at three positions starting at the center towards one of the corners. In case of high methane emissions, additional soil gas and microbial samples were taken at the respective spots.

For these eight wells, we established four different reference sites R1 to R4 (Figure 1). The reference grids consisted of nine measuring points covering an area of 20 x 20 m (Figure 2b). Measuring reference grids is necessary to determine and account for potential natural background variations for each abandoned well. Reference grids were typically located in a distance of ~~50~~15–150 m from the well site and on similar soil conditions and vegetation, and were investigated immediately after the measurement of the well grid. The reference site R4 for the abandoned well on the Meadow was measured once and the two reference sites for the wells in the Forest area (R1 and R2) were each measured twice on consecutive days (Table 2). The single reference site for the three wells in the Peat area (R3) was thus surveyed three times within one week. Three soil gas samples were usually taken in a diagonal pattern and the soil sample for microbial analysis in the center of the grid (Figure 2b). To estimate the general emission's spatial variability in the area, we sampled a transect through a point with high emission at the Peat reference site. The measuring points along the 12 m transect were 1 m apart.

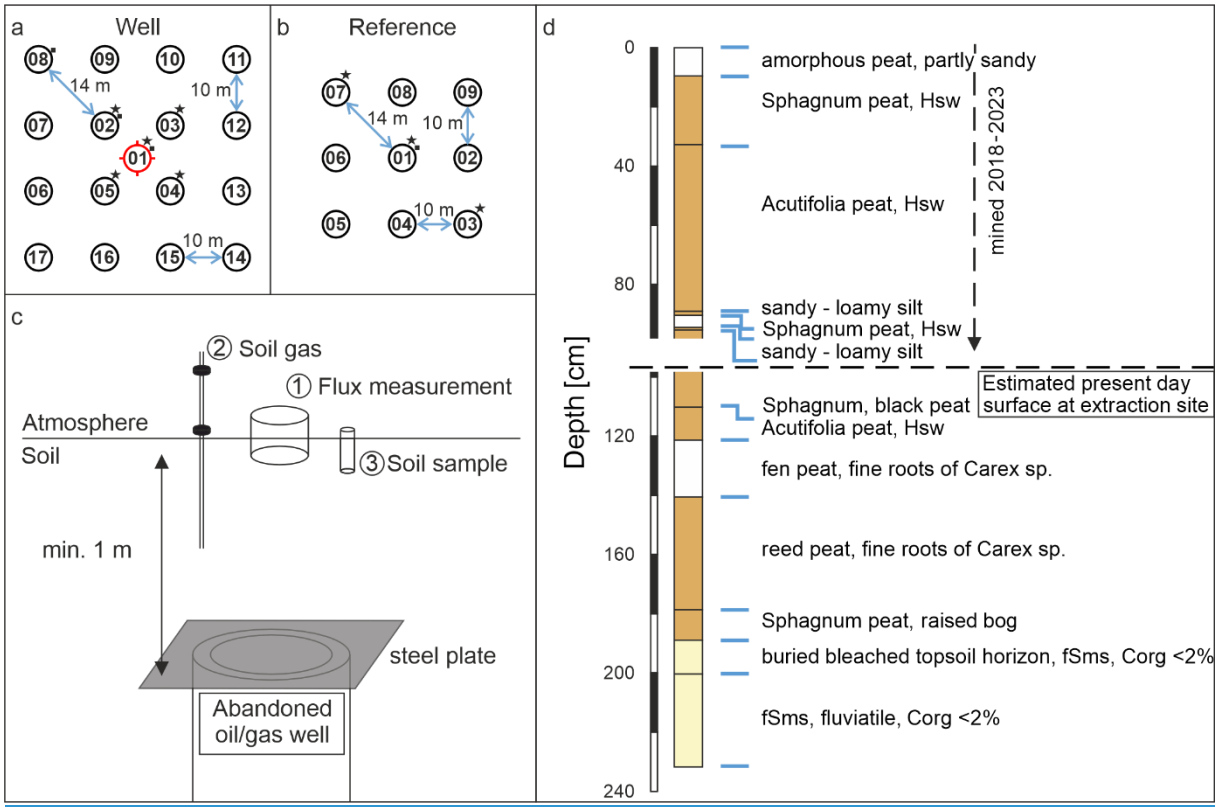
a
Well
08
09
10
11
14 m
10 m
07
02
03
12
01
06
05
04
13
10 m
17
16
15
14
b
Reference
07
08
09
14 m
10 m
06
01
02
05
04
10 m
03
c
② Soil gas
① Flux measurement
Atmosphere
Soil
③Soil sample
min. 1 m
steel plate
Abandoned
oil/gas well
d
Depth [cm]
0
40
80
120
160
200
240
amorphous peat, partly sandy
Sphagnum peat, Hsw
Acutifolia peat, Hsw
mined 2018 - 2023
sandy - loamy silt
Sphagnum peat, Hsw
sandy - loamy silt
Estimated present day
surface at extraction site
Sphagnum, black peat
Acutifolia peat, Hsw
fen peat, fine roots of Carex sp.
reed peat, fine roots of Carex sp.
Sphagnum peat, raised bog
buried bleached topsoil horizon, fSms, Corg <2%
fSms, fluviatile, Corg <2%

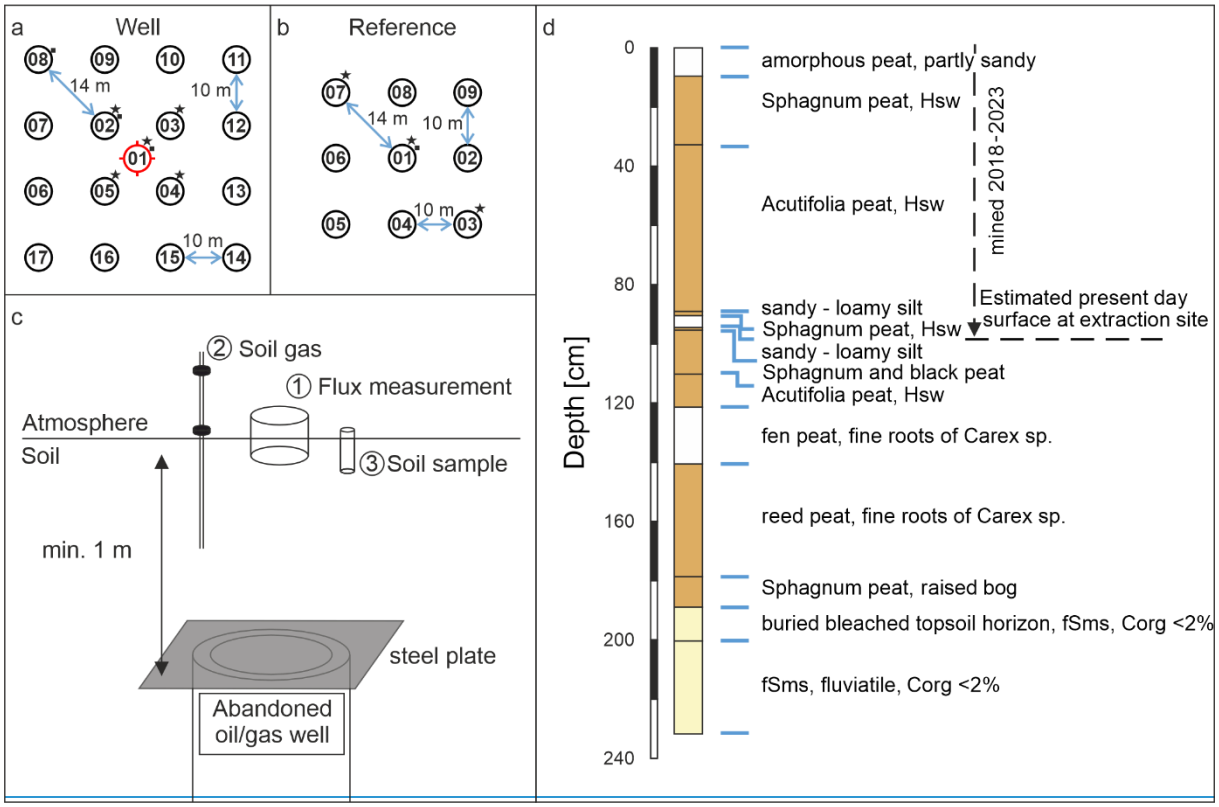

Figure 2: Sampling scheme for emission measurements (CH4 and CO2) for well (a) and close-by reference sites (b), both with likely similar biogeochemistry and vegetation, as well as a schematic display of a buried abandoned well (c, not by scale). Additional soil gas samples (stars) and soil samples for microbial analysis and methane oxidation rates determination (squares) were taken at the marked positions. The shift of the symbols towards the upper right was made for graphical reasons. Samples were directly taken on the numbered positions. The well position is marked in red. d) A simplified profile of a pedological well (# 54315, #54315, source LBEG) drilled in 1983 before peat extraction initiated. Coordinates RW: 32525578, HW: 5836405 (EPSG 4647), close (50 m west) to the reference grid in the peat extraction site. fSms: medium sandy fine sand, Hsw: diffuse or in nests enriched with unconsolidated sesquioxides. Link to map https://nibis.lbeg.de/cardomap3/?permalink=2RfGItuF.

2.3 Methane and CO2 carbon dioxide emission

Methane emissions from the soil surface into the atmosphere were measured with an optical feedback – cavity enhanced absorption spectroscopy trace gas analyzer (LI-COR 7810) coupled to a portable hydraulic chamber (LI-COR smart chamber) following the closed chamber principal. The measurement was conducted as instructed by the manufacturer, which is described in the following: First, defined plastic collars with a diameter of 20.3 cm and height of 12.4 cm (outside diameter 8.4", height 4.5") were positioned at each of the measuring points and were pushed few centimeters into the soil to guarantee a complete closure of the smart chamber with the underlying soil profile. Since the exact penetration depths of the collars were needed for the calculation of fluxes (dead volume of the ring) each insertion depth were measured individually.

After both devices, analyzer and chamber, reached operation modus, a startup measurement (triplicate) was conducted to ensure stable condition of the instrument. Each grid position was sampled in triplicates at least 1 h after placing the respective collar. ~~Therefore, t~~The chamber stayed closed for the time of one measurement (~~-~~120 s) to record continuously (1 Hz) the change in methane and carbon dioxide concentrations in the loop headspace, which was open to the soil surface. ~~Between measurements, the chamber stayed open for 60 s to enable equilibration with atmospheric CH_4 and CO_2 concentrations.~~ Gas fluxes were computed after a dead band time of 40 s after chamber closing, applying a linear regression of the concentration data for each singular measurement, subsequently averaging the triplicate measurements. Between measurements, the chamber stayed open for 60 s to enable equilibration with atmospheric CH_4 and CO_2 concentrations. Examples for such measurements and their r^2 are shown in the supplements (Supplement S1) and th~~T~~he standard deviation of the triplicate measurements is tabulated in supplementary data (Table S2).

Additional measurements at each site included soil moisture (SWC) and bulk conductivity measurements (EC) using a Stevens HydraProbe sensor with 6 cm long measuring rods. The sensor was not particularly calibrated for the organic (peat) rich soils at the study site and used the default "sand" settings for data evaluation. Thus, reported SWC and EC data in Table S2 are only indicative data. Since the short rods measured the temperature effectively directly below the soil surface with all potential bias to solar radiation, we applied an additional 25 cm long temperature probe (Omega, Type E) to better constrain soil temperatures. In addition, accompanying weather data, measured with a handheld device (e.g., temperature, wind speed and humidity) can be found in Table S8.

2.4 Soil gas sampling and compositional analysis

Gas samples were acquired using soil gas probes. The probes are made of stainless steel with an outer diameter of 6 mm and inner diameter of 3 mm with a total length of 1.5 m. To prevent the probes from becoming blocked while pushing into the ground, a pin has been attached to the front of the probe. This pin remains in the ground after the desired depth is reached and the probe was lifted by a few cm. The lances are usually driven into ground with a moveable anvil. However, ~~at the study site with soft unconsolidated sediments~~ they could easily be pushed into the maximum depth of 1 m at study sites with soft unconsolidated soils. Locations sampled are indicated in Fig. ~~2~~ 3 and wherever methane emission was detected. Due to the shallow ground water table, the probes often had to be lifted close to the surface to be able to sample the gas phase of the vadose zone, thus giving an ~~true~~approximate indication of the actual water level (sampling depths are listed in Table S1). A septum port is attached to the end of the probe, which allows sampling with a syringe. Before sampling, the dead volume of the soil gas probe was flushed twice with soil gas immediately after placement with a 20 mL syringe and then rested at least for 1 h to equilibrate. Afterwards 20 mL soil gas was extracted and stored in crimped vials pre-filled with saturated NaCl as sealing solution. Vials were stored upside down for a maximum of about two weeks before~~for~~ further gas analysis in the laboratory.

Stored gas samples were analyzed in the lab using a gas chromatograph (GC) Trace 1310 GC (Thermo Fischer Scientific, USA) equipped with a heated valve system and column switching. One milliliter of sample was then injected into the sample loops. The individual components were quantified in parallel on three channels.

On channel 1, pre-separation of hydrocarbons (C_1 through C_6) from a 500 µL sample was performed on a non-polar polysiloxane polymer column (Restek MX-1, 15 m, 0.28 mm ID, film thickness 3 µm). Molecular weight components $>C_7$ were back-flushed. Full separation was performed on the main 50 m Al_2O_3 capillary column (0.32 mm ID, film thickness 5 µm). Both columns were operated non-isothermally starting at 30 °C°C and ending at 180 °C°C. All components were detected on a Flame Ionization Detector (FID) with helium (He) as carrier gas.

On channel 2, the sample was injected via a 500 µl sample loop. CO_2 was separated from other components by a pre-column (30 m Hayesep Q, 0.53 mm ID, film thickness 20 µm) and directly detected after bypassing the Molsieve column on the thermal conductivity detector (TCD). All other components (Ne, H_2, Ar, O_2, N_2, CH_4, and CO) were chromatographically separated on the main analytical Molsieve column (80 m 5 Å, 0.53 mm ID, film thickness 50 µm). Carrier gas on this channel was He.

For better sensitivity for helium and hydrogen, these compounds were analyzed on a channel 3 with argon as carrier gas. The sample loop used had a volume of 125 µl. CO_2 and higher molecular weight carbon-components were retained and back-flushed on a packed pre-column (2 m Hayesep Q, mesh 100/120, 1 mm ID). Separation of He, Ne, H_2, O_2, and N_2 components was performed on a 5 Å packed molecular sieve column (3 m, mesh 80/100, 1 mm ID) and subsequently detected on a TCD.

2.5 Isotopic analysis of methane and carbon dioxide

For samples with concentrations (>200 ppm), carbon isotope signatures of CH_4 ($\delta^{13}C$-CH_4) and CO_2 ($\delta^{13}C$-CO_2) were determined after injecting into a continuous flow GC-IRMS system (Agilent GC coupled to a Thermo Fisher Scientific MAT 253 via a GC-Combustion interface II/III). The different compounds were separated on a 25 m Porapak column and methane was combusted to CO_2 at a temperature of 960 °C°C. Low concentration samples (2 – 200 ppm CH_4) were measured applying a cryo-focusing with liquid nitrogen of methane on a 1 m 1/16 packed column installed in an Agilent 6890 GC likewise coupled to a Thermo Fisher Scientific MAT 253 via a GC-Combustion interface II/III. Deuterium isotope signatures of methane (δ^2H–CH_4) were determined by a similar GC-IRMS system (Trace GC and Isolink/ConFlow IV coupled to a MAT 253) if methane concentrations were above 2000 ppm. Methane was reduced to molecular H_2 at a temperature of 1420 °C°C. The reproducibility for $\delta^{13}C$ is ± 0.3‰ and for δ^2H–CH_4 ± 3‰. $^{13}C/^{12}C$ and $^2H/^1H$ ratios are presented in the standard δ-notation versus the reference standards Pee Dee Belemnite (VPDB) and Standard Mean Ocean Water (VSMOW), respectively (Coplen, 2011).

2.6 Methane oxidation rates

In the field, shallow soil samples (down to 20 cm) were obtained using a stainless steel push core with an inner Plexiglas liner. Exact coordinates and sampling depth are listed in the supplementary data (Table S4). Deeper samples (40–100 cm) were retrieved with the help of an Edelman auger as a 20 cm composite sample. Samples were kept, transported, and stored at 4–7 ~~°C~~°C until further processing. As next step, samples were homogenized and 5 g subsamples were collected and stored at –20 ~~°C~~°C for DNA extraction. For determination of potential aerobic methane oxidation rates (MOx) each sample~~d~~ was divided into seven aerobic incubations (100 mL vials), with ~10 g homogenized soil sample in each. Three parallels were incubated with 1% methane in the headspace, four without methane with one being autoclaved prior to incubation.

Headspace methane and carbon dioxide concentration were determined regularly with a 610C gas chromatograph (SRI Instruments Europe GmbH, Bad Honnef, Germany) equipped with a flame ionization detector (FID) ~~and a copper methanizer to convert CO_2 to CH_4~~. At the end of the incubations, ~~active~~ bottles with active soil samples were subsampled for DNA extraction again (s. section DNA extraction) and then the remaining sample was dried at 80 ~~°C~~°C to calculate soil water content. In the end, methane oxidation was calculated as the slope of the declining methane concentration in µmol per incubation over time in a linear section of the graph. Subsequently, it was then accounted for the dry weight in case of MOx dry and the wet weight for MOx wet. Finally, to compare it to methane emissions MOx wet was multiplied by the respective soil density and a volume of 0.2 m^3, because 20 cm was the maximal depth of a composite sample.

2.7 DNA extraction

DNA was extracted from soil samples (~0.5 g) using the FastDNA SPIN kit for soil (MP Biomedicals, Illkirch, France). The extraction followed manufacturer's instructions with modifications as previously described Webster et al. (2003): (1) the addition of 200 µg of poly(adenylic acid) (Roche Diagnostics International Ltd., Rotkreuz, Switzerland) prior to bead beating; (2) two bead beating steps of 45 s at 6.5 m s^{-1} were performed on a FastPrep-24 system (MP Biomedicals); and (3) DNA was eluted in TE-buffer and quantified with the Quantifluor dsDNA chemistry using a Quantus fluorometer (Promega GmbH, Walldorf, Germany).

2.8 Sequencing bacterial and archaeal community via 16S rRNA genes

Following DNA extraction, samples were sequenced by Microsynth AG (Balgach, Switzerland) using MiSeq Illumina technology for microbial community analysis. Both ~~Bacteria~~ bacteria and ~~Archaea~~ archaea were sequenced from the same DNA extractions and analyzed separately by targeting the 16S rRNA gene. For bacteria primer pair 515F / 806R (GTG CCA GCM GCC GCG GTAA; GG ACT ACH VGG GTW TCT AAT; Caporaso et al. 2011) and for archaea 340F / ARCH806R (CCC TAY GGG GYG CAS CAG; GGA CTA CVS GGG TAT CTA AT; Takai and Horikoshi 2000; Gantner et al. 2011)

were used. Sequences will be deposited in the European Nucleotide Archive (ENA) and the accession number will be published in the final version of the manuscript. Sequences were processed following a bioinformatics pipeline (USEARCH, Edgar 2010; Cutadapt, Martin 2011; MOTHUR, Schloss et al. 2009) previously described by Dohrmann and Krüger (2023). Thereby ~~to generate~~ zero-radius OTUs (ZOTUs) ~~, (Edgar 2016) ,~~ are generated from OTUs using the UNOISE algorithm, which enable higher resolution with the goal to report all correct biological sequences (Edgar 2016). Potentially methanotrophic ZOUTs were identified according to the *pmoA* database taxonomy (Yang et al., 2016) and known methanotrophic genera (Knief, 2015, 2019 and references therein). Relative abundances of a methanotrophic genus or family were calculated as the share of all methanotrophic genera or families in the respective sample pool.

2.9 Quantification of methane oxidizing bacteria by *pmoA*-gene targeted quantitative PCR

Using ~~a~~ quantitative PCR (qPCR) assays to targeting both, general bacterial 16S rRNA gene and the *pmoA* gene encoding for the ß subunit of the particulate methane monooxygenase expressed by methane oxidizing bacteria (MOB), we were able to determine the methanotrophic abundances.

The qPCR targeting the 16S rRNA gene (primer pair 341F/ 805R; forward: 5′-GTGCCAGCMGCCGCGGTAA-3′, reverse: 5′-GGACTACHVGGGTWTCTAAT-3′) was performed as described previously (Hedrich et al., 2016). The *pmoA* gene targeting qPCR (primer pair 189F/ mb661r; forward: 5′-GGNGACCGGGATTTCTGG-3′, reverse: 5′-CAGGMGCAACGTCYTTACC-3′; Costello and Lidstrom 1999) was performed in a CFX Connect real-time PCR system (Bio-Rad, Hercules, CA) in a final volume of 10 µl, consisting of 5 µl 2x Luna Universal qPCR Master Mix (New England BioLabs GmbH, Frankfurt am Main, Germany), 0.7 µl forward and reverse primers each (10 µM), 0.5 µl bovine serum albumin (1 %), 1.1 µl nuclease-free water and 2 µl template DNA. The thermal profile consisted of an initial denaturation step at 95 ~~°C~~°C for 5 min, 40 cycles of denaturation at 95 ~~°C~~°C for 30 s, annealing at 62 ~~°C~~°C for 30 s, elongation at 72 ~~°C~~°C for 45 s, and an additional data acquisition step at 79 ~~°C~~°C for 8 s, followed by final elongation at 72 ~~°C~~°C for 5 min. The template DNA was used in five times or ten times dilution and spiked with the standard to a concentration of 10^5 copies per µl to correct for inhibition. Standards consisted of a dilution series (10^1 – 10^6 *pmoA* gene copies) of a PCR product flanking the *pmoA* gene of *Methylomonas rhizoryzae* GJ1 (Japan Collection of Microorganisms, JCM 33990) amplified with a designed primer pair (forward: 5'-GTACGCATACGCATGAACGC-3', reverse: 5'-GTTTCCCGTGCGTTTGACTG-3'). The amplicon specificity was confirmed using a melt curve and agarose gel electrophoresis. Samples that did not show this specificity, i.e., Forest samples, were not considered to calculate *pmoA* abundances.

3 Results

3.1 Methane emission

~~To investigate methane emissions related to abandoned onshore wells eight cut und buried wells in the south-eastern part of the oil field Steimbke-Nord covering an area of ~ 0.2 km² (Figure 1) were targeted. Three wells (R-WA 272, R-WA 254, R-WA 264) are located in the western part of the area where active peat mining is ongoing.~~ ~~Before the peat extraction in the active area began, the Peat site was also an agricultural meadow that was probably regularly fertilized with manure.~~~~One well (R-WA 275), ~ 350 m to the east, is located on a meadow which is temporarily grazed and possibly fertilized with liquid manure.~~ ~~Before the peat extraction in the active area began, the Peat site was also an agricultural meadow that was probably regularly fertilized with manure.~~ ~~Two of the four wells from the Forest area (dominated by birch trees and pines) are located between the active Peat site and the Meadow (R-WA 273, R-WA 274), the remaining two in a larger forested area ~ 225 m to the north and northeast, respectively.~~

~~For these eight wells, we established four different reference sites R1 to R4 (Figure 1). The reference site R4 for the abandoned well on the Meadow was measured once and the two reference sites for the wells in the Forest area (R1 and R2) were each measured twice on consecutive days (Table 2). The single reference site for the three wells in the Peat area (R3) was thus surveyed three times within one week.~~

In total 64 out of 206 single measurement points, from both well and reference sites, showed methane emissions to the atmosphere (Figure 3, Table S2). However, only 32 fluxes were higher than 1 nmol CH_4 m^{-2} s^{-1} and 31 of these were on the Peat sites. The absolutely highest flux was 540 nmol CH_4 m^{-2} s^{-1} on the Peat site (position 16, site R-WA 264) and the highest methane uptake was –4.4 nmol CH_4 m^{-2} s^{-1} at the Forest site R-WA 273, position 14 (Table S2). Compared to the Meadow site (~14%) and Forest sites (~15%) the Peats sites (~58%) had the highest number of sample points with methane emissions flux, too (Figure 3).

~~In total 64 out of 206 single measurement points showed methane emissions to the atmosphere, however, only the flux of 32 were higher than 1 nmol CH_4 m^{-2} s^{-1} and 31 of these were on the Peat site. The absolutely highest flux was 540 nmol CH_4 m^{-2} s^{-1} on the Peat site (position 16, site R-WA 264) and the lowest –4.4 nmol CH_4 m^{-2} s^{-1} at the Forest site R-WA 273 position 14 (Table S2).~~

The reference grid on the Peat site showed always (on three different measuring campaigns, Table S2) substantial methane emissions ranging from 15 to 380 nmol CH_4 m^{-2} s^{-1} but only at the northern and middle transect lines. The southern three points always represented a sink or the methane emissions were lower than 0.2 nmol CH_4 m^{-2} s^{-1}.

~~Thirteen out of 17 measuring points of the grid above well R-WA 275 on the Meadow and all corresponding reference measuring points were a methane sink (up to –1.2 nmol CH_4 m^{-2} s^{-1}). Only the four southernmost grid points at the well depict small methane emissions between 0.08 and 0.3 nmol CH_4 m^{-2} s^{-1}.~~

As a simple first approximation, we averaged all measuring points of the individual well and reference grids (mean and median, Table 2) with all the peat sites showing net methane emissions. The Peats reference sites had the highest mean emissions (~109

nmol m^{-2} s^{-1}). However, this should not be directly compared to more sophisticated emission techniques, e.g. long term eddy covariance studies, but rather as a snapshot of our study site for internal comparison of wells/references and different grounds (Forest, Meadow, Peat).

Mean and median values that are close to each other are typical for symmetrical distributions with minimal outliers. This holds for the data from the Forest and Meadow for both well and reference site (Table 2, Figure 4a, d). The data from the Peat sites show means that are much higher than medians indicating positively skewed data i.e. outliers on the high end (compare histogram Figure 4g). However, as such outliers can control the methane emissions of an area the mean is more suitable for an emission estimation. The difference between median and mean indicate the huge variation in methane emissions at the Peat sites, which is better visible in the Box-whisker plots (Figure 5). This is particularly evident at R-WA 264 with one grid point showing 560 nmol CH_4 m^{-2} s^{-1} and only two additional points with 30 nmol CH_4 m^{-2} s^{-1}. All other 14 values are negligible small positive or representing a sink. Thus, the median of this grid is negative whereas the mean is positive (38 nmol CH_4 m^{-2} s^{-1}).

As methane emissions did not show apparent differences between well and reference sites we first used the Kruskal-Wallis-Test to test for normal distribution, which the methane fluxes did not show. The Mann-Whitnes-U-test was then used to compare well and reference sites data. For R-WA 211, R-WA 209, R-WA 273, R-WA 264, R-WA 272, R-WA 275 well and reference sites were similar with regard to methane fluxes using this test. R-WA 274 and R-WA 254 showed significant differences in fluxes between well and reference sites. The reference site of R-WA 254 showed higher methane emissions than the well site. In case of R-WA 274 both sites were net methane sinks, however, the methane uptake of the well site was higher. The box-whisker plots (Figure 5, Table S9) depict this graphically. Especially, the huge differences between the Peat and the other sites is apparent.

Summarizing, all three well sampling grids, for which we observed overall methane emissions based on the mean values of 17 grid points covering an area of 900 m^2 around the well, were located in the Peat area. At wells R-WA 254 and R-WA 264 highly localized methane emissions with high flux rates occurred. These singular grid points with high methane emissions are not spatially correlated with the well location. Moreover, averaged methane emissions (both mean and median) were even consistently higher at the Peat reference site than well sites in the Peat area (Table 2). All four Forest wells were a stronger sink than the corresponding reference sites at the day of measurement. The Forest sites acted as a higher methane sink than the Meadow site.

In addition to these sampling grids, we sampled a transect through a point with high methane emissions (Figure 6). The resulting methane fluxes varied more than two orders of magnitude over the distance of less than one meter, whereas CO_2 emissions showed fewer changes and varied in total only by a factor of ~2.

~~All grid points of the wells R-WA 273 and R-WA 274 in the Forest between the Peat site and the Meadow were a methane sink ranging from -4.4 to -0.03 nmol CH_4 m^{-2} s^{-1}. Only the reference site (R2.1 and R2.2) showed methane emissions on three grid points at the southwestern edge consecutively on both measuring day (< 0.2 nmol CH_4 m^{-2} s^{-1}, Table S2, Figure 1). Well~~

sites and the reference site in the northern Forest do not reveal a pattern of methane emissions rates. A few grid points of the well areas (5 out of 34) revealed methane emissions with a singular value exceeding 1 nmol CH_4 m^{-2} s^{-1}.

Results from the well sites and single reference site on the Peat area are more variable. At well R_WA_264 high methane emission rates have been determined at the southwestern corner including the highest flux rate of 540 nmol CH_4 m^{-2} s^{-1}. The two nearest grid points to the west still revealed flux rate of ~ 30 nmol CH_4 m^{-2} s^{-1}, the highest flux was 540 nmol CH_4 m^{-2} s^{-1}, whereas all other points showed slightly positive to negative values. Four well grid points of R_WA_272 revealed high emission rates ranging from 40 to 160 nmol CH_4 m^{-2} s^{-1}, the highest flux was 540 nmol CH_4 m^{-2} s^{-1}, these are located at the northwestern part of the grid close to the reference grid ~ 50 m to the northwest. Similar to R_WA_264 all other points showed slightly positive to negative values. Two grid points of well R_WA_254 showed slightly elevated fluxes of ~7 nmol CH_4 m^{-2} s^{-1}, the remaining positive emissions being below 0.25 nmol CH_4 m^{-2} s^{-1} and all other measurements proving a strong methane sink, up to −2 nmol CH_4 m^{-2} s^{-1}.

The reference grid on the Peat site showed always (on three different measuring campaigns) substantial positive methane emissions ranging from 15 to 380 nmol CH_4 m^{-2} s^{-1} but only at the northern and middle transect lines. The southern three point always represented a sink or the emissions were lower than 0.2 nmol CH_4 m^{-2} s^{-1}.

As a simple first approximation, we averaged all measuring points of the individual well and reference grids (mean and median, Table 2). However, this should not be directly compared to more sophisticated emission techniques, e.g. long term eddy covariance studies, but rather as a snapshot of our study site for internal comparison of wells/references and different grounds (Forest, Meadow, Peat).

Mean and median values that are close to each other are typical for symmetrical distributions with minimal outliers. This holds for the data from the Forest and Meadow for both well and reference site (Table 2, Figure 3a, d). The data from the Peat site show means that are much higher than medians indicating positively skewed data i.e. outliers on the high end (compare histogram Figure 3g). However, as such outlier can control emissions of an area the mean is more suitable. On the other hand, the difference between these two indicate the huge variation in emissions at the Peat site. This is particularly evident at R_WA_264 with one grid point showing 560 nmol CH_4 m^{-2} s^{-1} and only two additional points with 30 nmol CH_4 m^{-2} s^{-1}. All other 14 values are negligible small positive or representing a sink, thus the median of this grid is negative whereas the mean is positive (38 nmol CH_4 m^{-2} s^{-1}).

Summarizing, all three well sampling grids, for which we observed overall methane emissions based on the mean values of 17 grid points covering an area of 900 m^2 around the well, were located in the Peat area. At wells R_WA_254 and R_WA_264 highly localized methane emissions with high flux rates occur. These singular grid points with high emissions are not spatially correlated with the well location. Moreover, averaged methane emissions (both mean and median) were even consistently higher at the Peat reference site than well sites in the Peat area (Table 1). All four Forest wells were a stronger sink than the corresponding reference sites at the day of measurement. The Forest's acted as a higher methane sink than the Meadow site.

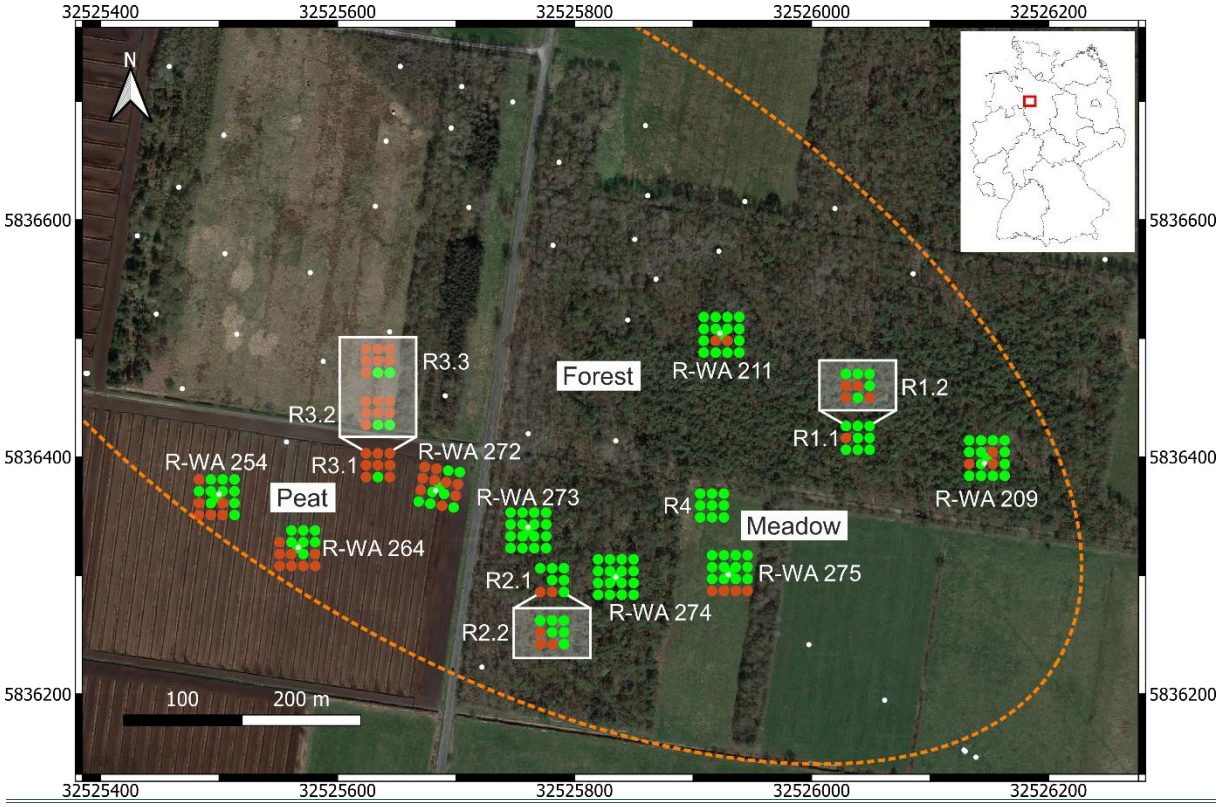

Figure 3: Overview of the study site indicating ~~in Steimbke~~ methane emissions (red) and methane uptake (green) for ~~with the~~ well sites (17 measuring points) and ~~and~~ reference sites (~~measuring grids each with 17 and~~ 9 measuring points), respectively. Abandoned wells are depicted in white dots. The rough dimensions of the oil field Steimbke-Nord are outlined ~~by the yellow~~ (orange dotted line). Coordinates are stated in UTM-32U (WGS84) with easting and northing planar coordinates in meter. ~~Green indicates negative methane emission (methane sink) whereas red indicates positive methane emission (methane source) for each flux measuring point.~~ The multiple measurements of reference sites are shown in a white box. The map was created using QGIS (v.3.22.3) and © Google Earth satellite images from 2015 as background.

Table 2: Summary of the sampled oil well and reference sites. The displayed natural fluxes are examples from literature (Abdalla et al. 2016, Oertel et al. 2016) as well as the emissions from abandoned wells, which were compiled from Williams et al. (2021) and Cahill et al. (2023).

short name	date	area	CH_4 flux [nmol m^{-2} s^{-1}] mean	median	mean soil CH_4 [ppm]	mean $\delta^{13}C$-CH_4 [‰]	mean δ^2H-CH_4 [‰]
R-WA 211	09.03.2022	Forest	–0.47	–0.13	1.4	–51	
R1.1		Forest	–0.12	–0.09	2.1	–49.6	
R-WA 209	10.03.2022	Forest	–0.35	–0.16	1.6	–56.3	
R1.2		Forest	–0.08	–0.05	2.1	–49.6	
R-WA 273	30.03.2022	Forest	–1.31	–1.22	1.4	–48.3	
R2.1		Forest	–0.76	–0.87	5.2	–56.1	
R-WA 274	31.03.2022	Forest	–1.41	–1.14	20.3	–61	
R2.2		Forest	–0.51	–0.43	6.7	–58	
R-WA 275	21.04.2022	Meadow	–0.2	–0.2	3,695	–85.4	–222.8
R4		Meadow	–0.1	–0.1	4,467	–99.1	–181.8
R-WA 272	20.04.2022	Peat	25.38	0.31	376,918	–58.4	–338
R3.1		Peat	50.07	15.42	181,802	–64.9	–306.9
R-WA 254	27.04.2022	Peat	0.25	–0.08	286,312	–66.1	–332.1
R3.2		Peat	109.03	55.79	369,909	–63.1	–316.3
R-WA 264	28.04.2022	Peat	37.56	–0.05	537,317	–64	–314.1
R3.3		Peat	50.5	20.91	290,555	–65.9	–304.1

short name	date	area	CH_4 flux [nmol m^{-2} s^{-1}] mean	median	mean soil CH_4 [ppm]	mean $\delta^{13}C$-CH_4 [‰]	mean δ^2H-CH_4 [‰]
R-WA 211	09.03.2022	Forest	–0.47	–0.13	1.4	–51	
R1.1		Forest	–0.12	–0.09	2.1	–49.6	
R-WA 209	10.03.2022	Forest	–0.35	–0.16	1.6	–56.3	
R1.2		Forest	–0.08	–0.05	2.1	–49.6	
R-WA 273	30.03.2022	Forest	–1.31	–1.22	1.4	–48.3	
R2.1		Forest	–0.76	–0.87	5.2	–56.1	
R-WA 274	31.03.2022	Forest	–1.41	–1.14	20.3	–61	
R2.2		Forest	–0.51	–0.43	6.7	–58	
R-WA 275	21.04.2022	Meadow	–0.2	–0.2	3,695	–85.4	–222.8
R4		Meadow	–0.1	–0.1	4,467	–99.1	–181.8
R-WA 272	20.04.2022	Peat	25.38	0.31	376,918	–58.4	–338
R3.1		Peat	50.07	15.42	181,802	–64.9	–306.9
R-WA 254	27.04.2022	Peat	0.25	–0.08	286,312	–66.1	–332.1
R3.2		Peat	109.03	55.79	369,909	–63.1	–316.3
R-WA 264	28.04.2022	Peat	37.56	–0.05	537,317	–64	–314.1
R3.3		Peat	50.5	20.91	290,555	–65.9	–304.1

natural forest flluxes	–1.9 to 23 nmol m^{-2} s^{-1-1}
natural grassland fluxes	–0.7 to 0.8 nmol m^{-2} s^{-1}
natural wetland fluxes	–0.5 to 650 nmol m^{-2} s
abandoned well fluxes	30 to 8 x 10^5 nmol m^{-2} s^{-1}

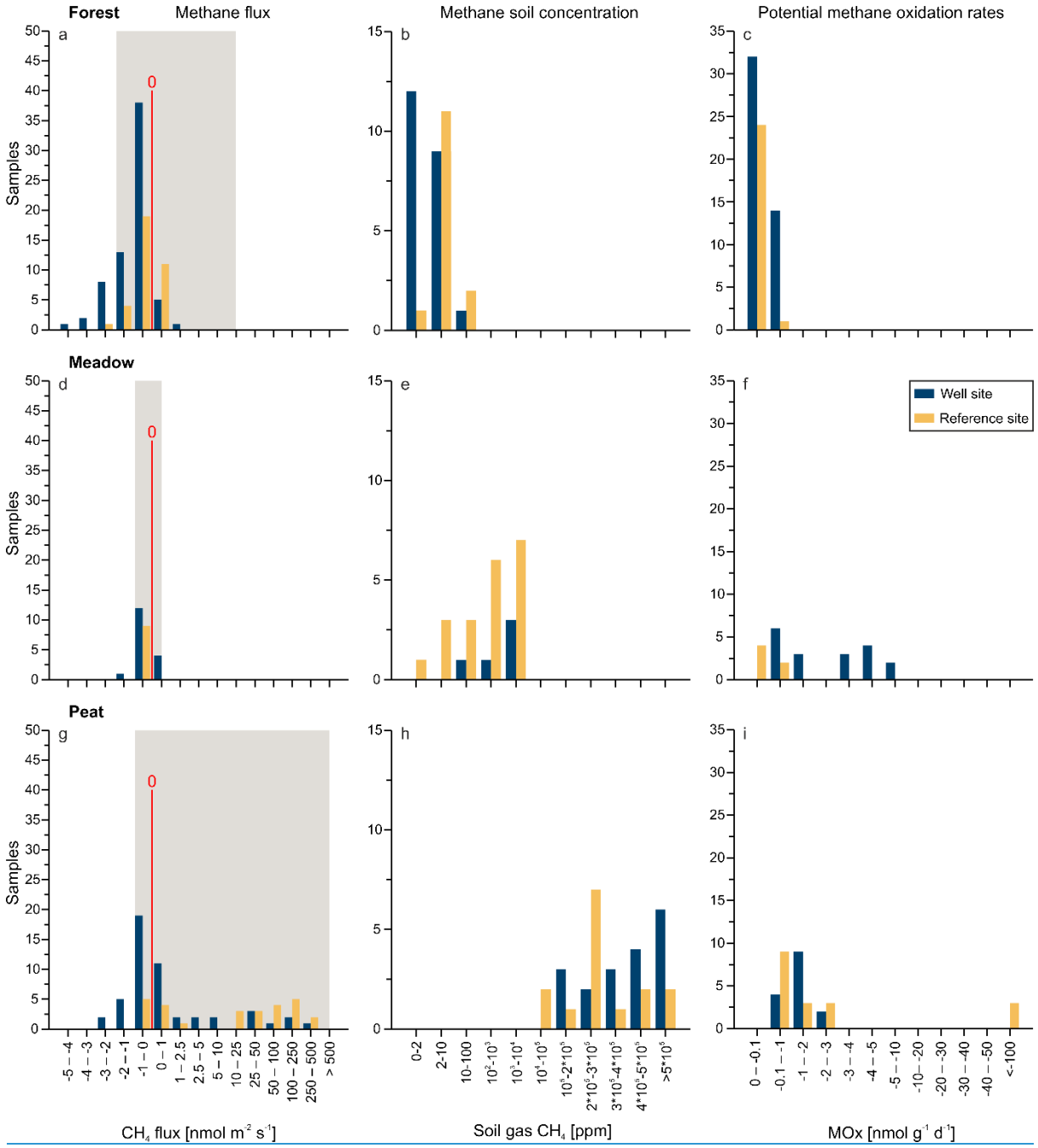
Forest
Methane flux
Methane soil concentration
Potential methane oxidation rates
Meadow
Peat
Samples
Well site
Reference site
CH4 flux [nmol m-2 s-1]
Soil gas CH4 [ppm]
MOx [nmol g-1 d-1]

494

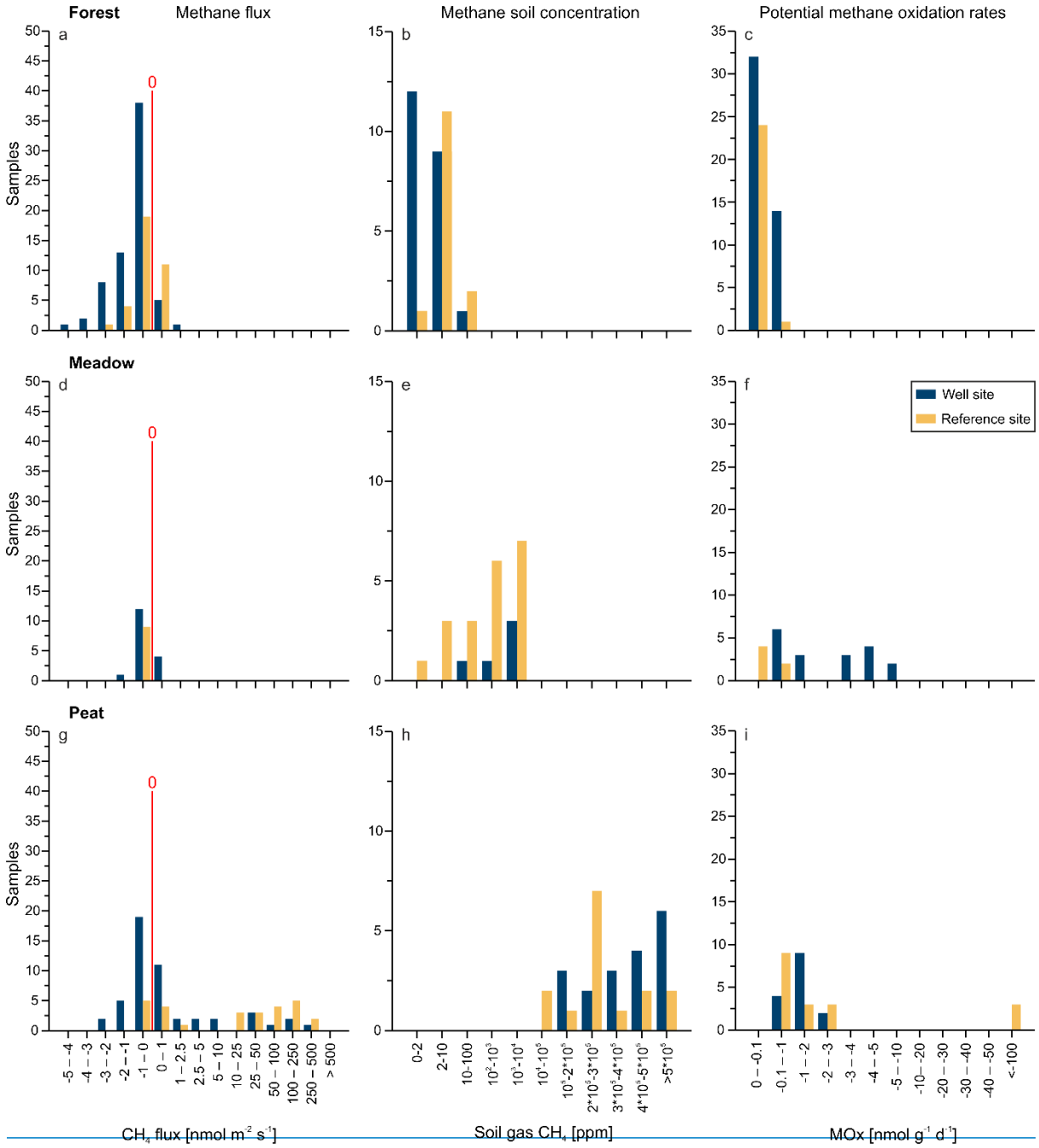

Figure ~~3~~4: Methane flux (a, d, g), soil gas methane concentration (b, e, h), and potential methane oxidation rates (MOx; c, f, i) depicted as histograms for well (blue) and reference sites (orange) at the three areas Forest (a, b, c), Meadow (d, e, f), and Peat extraction site (g, h, i). The red line in a, d, g indicates zero flux, sites left of the line acted as net methane sinks and at the right as net methane sources. The grey background represents natural ranges mentioned in literature (Abdalla et al. 2016, Oertel et al. 2016).~~Methane flux (a, d, g), soil gas methane concentration (b, e, h), and potential methane oxidation rates (MOx; c, f, i) depicted as histograms for well (blue) and reference sites (yellow) at the three areas forest (a, b, c), meadow (d, e, f), and peat extraction site (g, h, i). The red line in a, d, g indicates zero flux, sites left of the line acted as net methane sinks and at the right as net methane sources.~~

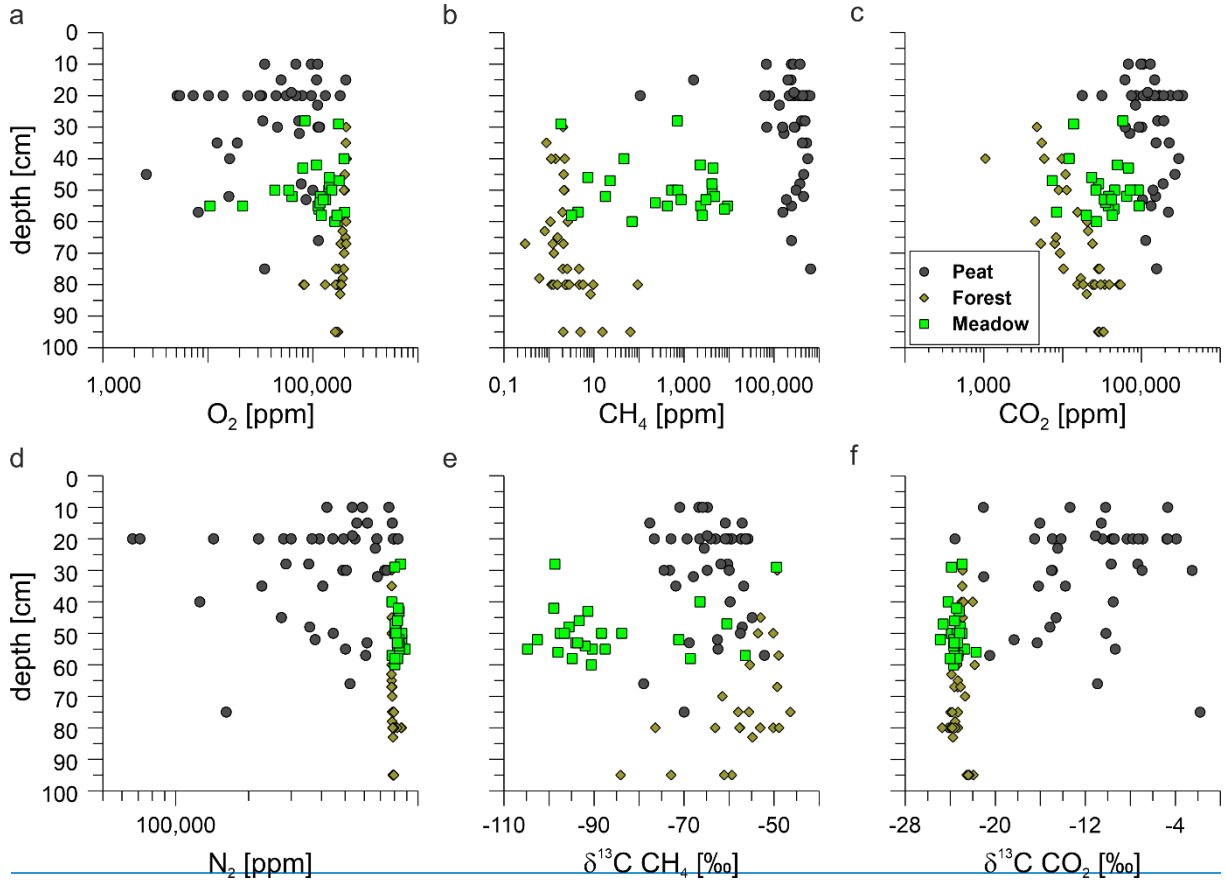

Figure 4: **Depth profiles of O_2 (a), CH_4 (b), CO_2 (c), and N_2 (d) soil gas concentrations, as well as $\delta^{13}C$-CH_4 (e) and $\delta^{13}C$-CO_2 (f) values for Forest (brown diamonds), Meadow (light green squares) and Peat (dark grey circles) sites.**

~~Note the logarithmic scales in a to f. Isotopic composition of methane (d) and carbon dioxide (c) is depicted as~~

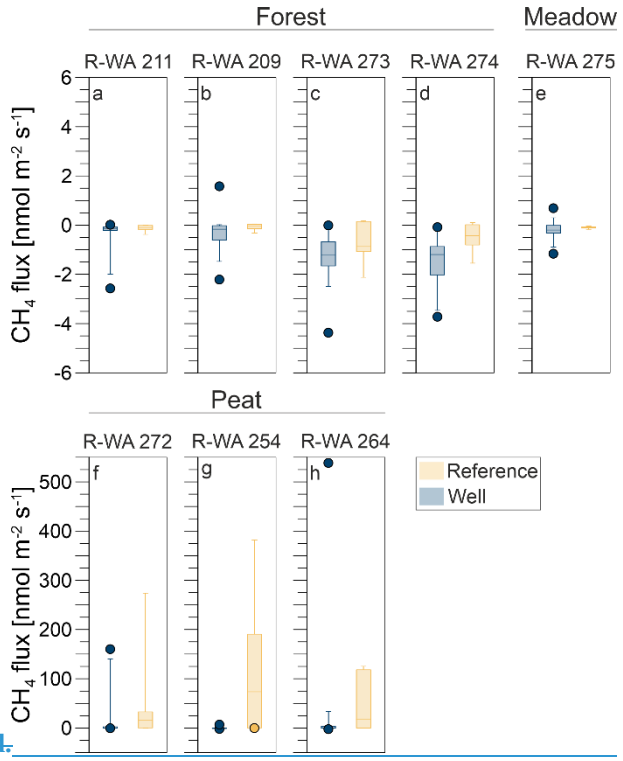

~~difference to the Vienna Pee Dee Belemnite (VPDB) standard.~~

Figure 5: Box-whisker plots (including outliers) of methane emissions from well (blue) and reference (orange) sites: Forest (a, b, c, d), Meadow (e), Peat (f, g, h). The underlying statistical parameters are listed in Table S9.

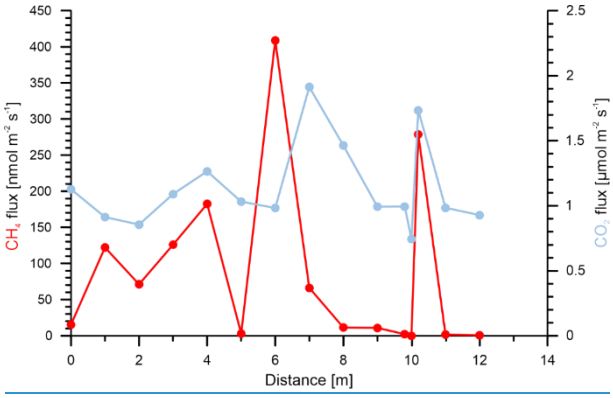

Figure 6: Methane (red) and CO_2 (blue) fluxes on a meter scale over a 12 m transect at the peat reference site. The fluxes were measured over the course of 3 h. Data is listed in Table S3.

3.2 Soil gas geochemistry

Soil gas samples were taken from up to 95 cm depth and analyzed in the laboratory for gas compositions including gaseous hydrocarbons (C_1–C_6) as well as carbon and hydrogen isotopic composition if ~~possible~~concentrations were sufficient. Depths of the soil gas sampling differed and were ~~determined~~ limited by the depth of the groundwater table at the time of sampling. Generally, the sampling depth was closely above the groundwater table and is, thus, an indirect measure of the ~~lowest~~ deepest interval of the vadose zone at the time of sampling. The soil methane concentrations between the sampled areas were clearly distinct, with Forest soils showing the lowest methane concentrations compared to Meadow and Peat (extraction site) soil gases (~~Figure 3~~Figure 4b, e, h and 7~~4~~b). The majority of methane concentrations at the Forest sites were around or below atmospheric concentrations (Table S1), however, two samples had with ~93 ppm and ~64 ppm elevated methane concentrations. These Forest sites did not emit substantial amounts of methane (Table 2~~1~~). The overall mean for samples from Forest soil was ~7.5 ppm methane (Table S1), the median however was ~2.1 ppm~~, which corresponds to atmospheric concentrations~~. Soil methane concentrations in samples from the nearby Meadow site started at ~1.8 ppm and reached up to 9,200 ppm. The respective mean methane concentration was ~1,960 ppm and the median ~710 ppm. Soil gas samples from the Peat ~~(~~extraction site~~)~~ showed both, the highest overall concentration with nearly 65% methane (~645,000 ppm) and with ~315,000 ppm (mean) and 282,000 ppm (median) the highest mean and median concentration, respectively. The general differences in the soil gas composition between the three sampling areas becomes also clear from the plot of ~~all data on~~ O_2, CH_4, CO_2, and N_2 concentrations with depth (Figure ~~4a~~7a–d).

We also analyzed the $\delta^{13}C$-CO_2, $\delta^{13}C$-CH_4, and $\delta^{2}H$-CH_4 for most soil gas samples (Table S1). Methane concentrations in the Forest soil were, however, too low to determine $\delta^{2}H$-CH_4. As for $\delta^{13}C$-CO_2, isotopic compositions' of Forest and Meadow soil gases were similar, ranging both between –21.7‰ and –24.9‰ (Figure 7)~~, with means of ~ –23.3‰ and ~ –23.5‰, respectively~~. Soil gases from the Peat site, on the contrary, were much more ^{13}C-enriched with $\delta^{13}C$ values up to –1.8‰ and a mean of ~–11.6‰. Thus, while for the Forest and Meadow area $\delta^{13}C$-CO_2 in the soil gas was relatively uniform and typical for common soil gas, variations at the Peat extraction sites were high, indicative for different controls on soil CO_2 in this area (Figure 7~~4~~f). The $\delta^{13}C$-CH_4 signatures differed between all three areas with the methane in the Meadow soil being most ^{13}C-depleted with a mean $\delta^{13}C$ value of ~~~~–86.6‰ ~~(–104.8‰ to –49.5‰)~~, in the Forest soil of ~~~~–57.4‰ ~~(–84.1‰ to 46.4‰)~~, and in Peat soil of ~~~~–63.8‰ ~~(–79‰ to –52.2‰; see also (~~Figure 4e7e). The mean hydrogen isotopic composition of methane differed strongly between the Meadow and Peat soil gases with $\delta^{2}H$-CH_4 of ~~~~–270‰ and ~~~~–320‰, respectively (Table S1). All isotope data from the reference and well sites were not systematically different from each other~~did not show any relevant differences~~.

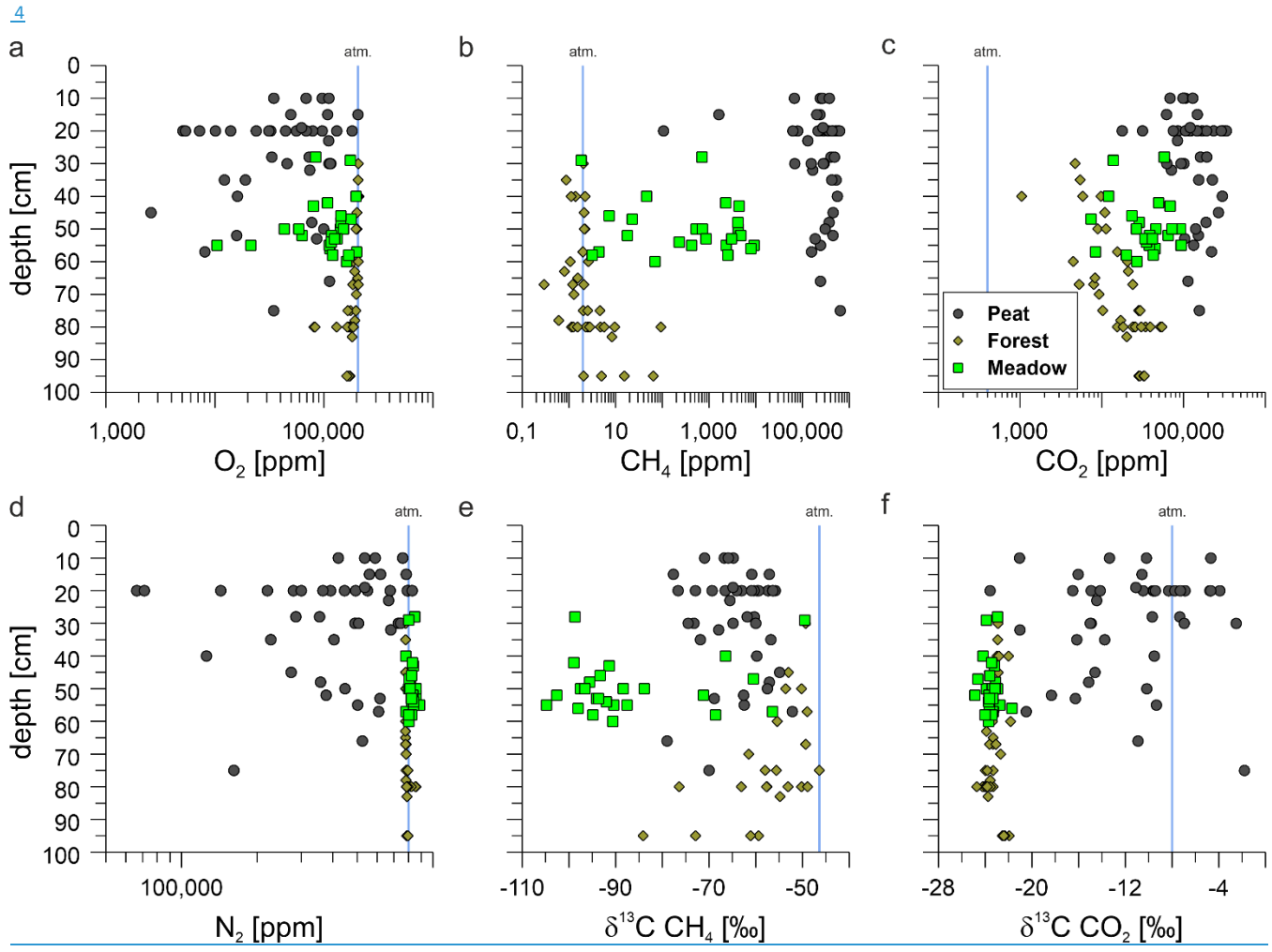

Figure 7: Depth profiles of O_2 (a), CH_4 (b), CO_2 (c), and N_2 (d) soil gas concentrations, as well as $\delta^{13}C$-CH_4 (e) and $\delta^{13}C$-CO_2 (f) values for Forest (brown diamonds), Meadow (light green squares) and Peat (dark grey circles) sites. Atmospheric values are depicted as blue lines. Note the logarithmic scales in a to c. Isotopic composition of methane (e) and carbon dioxide (f) is depicted relative to the Vienna Pee Dee Belemnite (VPDB) standard.

3.3 Methane oxidation rates

Methane oxidation rates were determined to investigate the soils' potential to mitigate methane emissions. In total 27 positions were sampled in up to two depths, resulting in 46 methane oxidation rates. ~~Following the incubations, the potential oxidation rates were determined per gram dry soil. In addition, we calculated methane oxidation rates for a square meter of wet soil with 20 cm height, which was the maximum aggregated depth for a homogenized soil sample. This way, we got interpolated~~

~~methane oxidation rates for the sampled soil column that are considered better comparable with measured and published methane fluxes (e.g. calculated per well).~~

Mean methane oxidation rates per g dry soil (Table 3) were lowest for Forest soils (~ 0.04 nmol g^{-1} s^{-1}) and highest for soils from the Peat sites (~18.3 nmol g^{-1} s^{-1}) with intermediate values for Meadow soils ~~(1.4 nmol g^{-1} s^{-1})~~. To get an estimate of actual oxidation rates in the soil column, we calculated the ~~Potential~~ potential methane oxidation rates per g wet soil sample and a height of 20 cm (Table 3,~~single measurements:~~ Table S4). These rates followed the same pattern as the dry methane oxidation rates and methane soil concentrations and were highest in the industrial Peat area. ~~ranged between 2 nmol 0.2 m^{-3} s^{-1} and ~266 nmol 0.2 m^{-3} s^{-1} in Forest soils, ~11 nmol 0.2 m^{-3} s^{-1} and ~8383 nmol 0.2 m^{-3} s^{-1} at the Meadow, and ~81 nmol 0.2 m^{-3} s^{-1} and ~150,000 nmol 0.2 m^{-3} s^{-1} at the industrial Peat site. The respective mean oxidation rates per g wet soil sample (Table 3) for the three studied areas increased from ~47 nmol 0.2 m^{-3} s^{-1} (Forest) over ~3100 nmol 0.2 m^{-3} s^{-1} (Meadow) to ~14,100 nmol 0.2 m^{-3} s^{-1} (Peat extraction site). Mean dry MOx are listed in Table 3.~~

Table 3: Mean areal methane oxidation rates (MOx) for Forest, Meadow and Peat sites calculated per gram dry soil as well as for dry and wet soil of a volume of 1 m^2 and 0.2 meter height (= 0.2 m^3) as well as mean 16S-RNA gene and *pmoA* abundance per gram dry soil. *pmoA* abundance was calculated as relative to 16S rRNA gene abundances.

	MOx dry [nmol CH_4 g^{-1} s^{-1}]	MOx dry [nmol CH_4 0.2 m^{-3} s^{-1}]	MOx wet [nmol CH_4 0.2 m^{-3} s^{-1}]	16S rRNA gene [10^9 g^{-1} dry wt.]	*pmoA* [10^6 g^{-1} dry wt.]	*pmoA* abundance [%]
Forest	0.04	85	47	13		
Meadow	1.4	2475	3106	16	30	0.19
Peat	18.3	18199	14114	4.6	14	0.30

For a selected experiment on the methane turnover in the Peat area the carbon isotopic fractionation of methane during aerobic methane oxidation was determined in the laboratory (see supplement ~~S2~~S3). Using a calculation from (Feisthauer et al., 2011) this resulted in an epsilon (ε) of –31.3‰ (~~Table~~ Supplement ~~S2~~S3).

~~3.4 MOB abundance and identification~~

~~We determined MOB abundances by targeting both, the general 16S rRNA gene and *pmoA* gene using qPCR (Table 3). The Peat sites had with ~4.6 x 10^9 copies g^{-1} dry weight about three times lower 16S RNA gene copies than the other two sites with 1.3 x 10^{10} (Forest) and 1.6 x 10^{10} copies g^{-1} dry weight. The *pmoA* abundances were similar at Meadow and Peat site, with 3.0 x 10^7 and 1.4 x 10^7 copies g^{-1} dry weight, respectively. The relative abundance of the *pmoA* was highest in the Peat (~0.30%) reaching up to 0.89%, followed by the Meadow (0.19%). However, there were huge differences between the samples in each area (Table S5).~~

~~We used DNA based microbial analyses to identify changes in bacterial community over depth and identify potential methanotrophic key player. Bacterial 16S rRNA gene sequencing revealed between ~1.5 x 10^4 and ~1.35 x 10^5 sequences per~~

sample with a median of ~8.5 x 10^4 sequences and a mean library coverage C of >98.5% (data not shown). In total ~22 x 10^4 ZOTUs were determined. A comparison on genus level with published taxa known to contain the *pmo operon* sequences resulted in up to 151 potential methanotrophic ZOTUs, grouping into 15 methanotrophic genera and 5 families (Table S6). The most abundant putative methanotrophic family in amplicon libraries was *Methylacidiphilaceae*, with 71 uncultured ZOTUs followed by *Beijerinckiaceae*. The most abundant genera were *Methylocystis* and the uncultured cluster SH765B-TzT-35 from the *Methylomirabilaceae* family (hereafter referred to as SH765B-TzT-35). In the following, we grouped the ZOTUs belonging to the same genera together in order to simplify the dataset and make changes between the areas better visible.

Most reads affiliating with known methanotrophic taxa reads were found at the Peat site, whereas Forest and Meadow had about half as much reads. In Forest samples, most of such reads were found in the top layer. On the contrary, they increased with depth for the Meadow site until a depth of 8–13 cm and 15–20 cm at the Peat site and decreased afterwards in both cases slightly (Table S6). The top layer at Forest and Meadow sites was with regard to methanotrophic taxa dominated by an uncultured *Methylacidiphilaceae* genus, which relative share in reads decreased with depth but was still the most abundant genus (Figure 5). A member of the genus *Methylocystis*, however, dominated the peat site, its relative abundance first increased to a depth of 20 cm and the abruptly declined at a depth of more than 40 cm. In samples of 40 cm and below SH765B-TzT-35 dominated the methanotrophic community (Figure 5).

In addition to bacterial 16S RNA gene sequencing, we used archaeal primer to identify methanogenic key player. Sequencing resulted into ~9.3 x 10^3 and ~ 1.2 x 10^5 reads per sample with a coverage of >99.9% (data not shown). Overall, 798 ZOTU were identified and a comparison with known methanogenic genera revealed 132 potential methanogenic ZOTU (Table S7). These could be grouped into 11 genera and 9 families (Figure 5). The most abundant genera were *Methanosarcina*, followed by *Methanoregula*, which was almost exclusive present in Peat samples, and third *Methanosaeta*. Together with *Methanobacterium* they account for 96% of methanogenic reads over all samples.

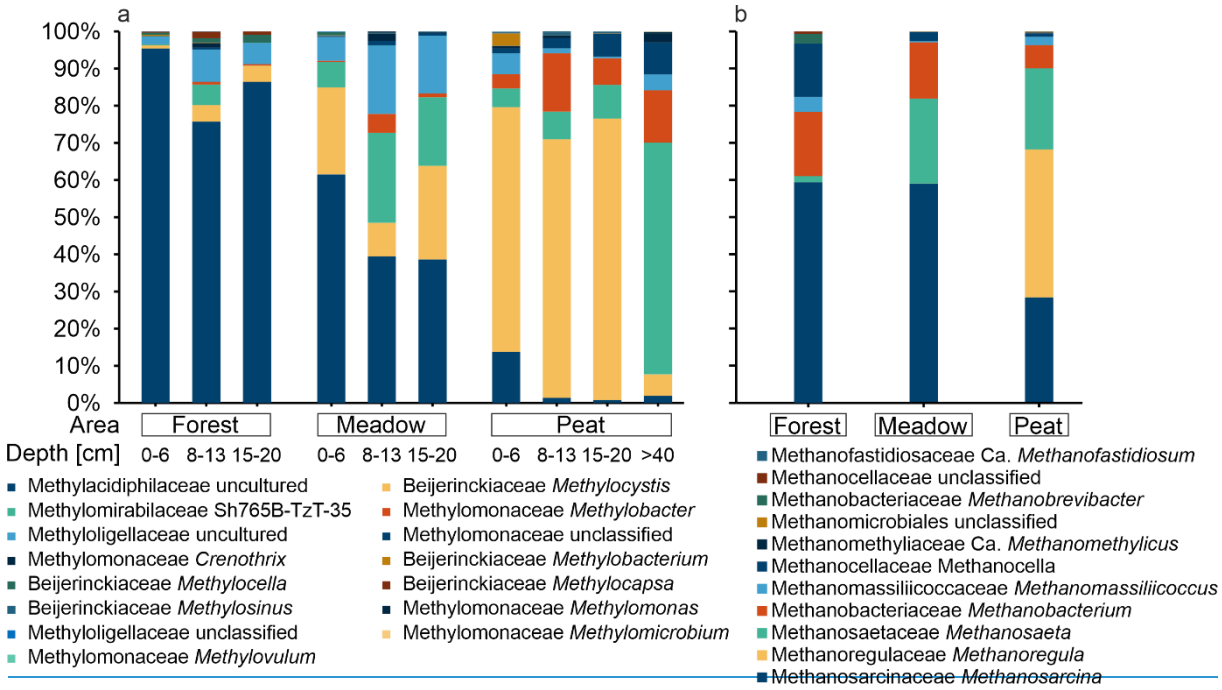

Figure 5: a) Relative abundance of potential methanotrophic genera estimated at three depth intervals detected in the Forest, Meadow, and at four depth intervals in the Peat areas. b) Potential methanogenic genera detected at the three areas Forest, Meadow, and Peat depicted as relative abundance. Reads are displayed as relation to the sum of all reads associated with methanotrophic taxa in the respective sample pool.

3.4 MOB abundance and identification

We determined MOB abundances by targeting both, the general 16S rRNA gene and the for the methanotrophic bacteria specific *pmoA* gene using qPCR (Table 3). The Peat sites had with ~4.6 x 10^9 copies g^{-1} dry weight about three times lower 16S RNA gene copies than the other two sites with 1.3 x 10^{10} (Forest) and 1.6 x 10^{10} (Meadow) copies g^{-1} dry weight. The *pmoA* gene abundances were similar at Meadow and Peat site, with 3.0 x 10^7 and 1.4 x 10^7 copies g^{-1} dry weight, respectively. The relative abundance of the *pmoA* gene was highest in the Peat (~0.30%) reaching up to 0.89%, followed by the Meadow (0.19%). However, there were huge differences between the samples in each area (Table S5).

We used DNA-based microbial analyses to identify changes in bacterial community over depth and identify potential methanotrophic key players. Bacterial 16S rRNA gene sequencing revealed between ~1.5 x 10^4 and ~1.35 x 10^5 sequences per sample with a median of ~8.5 x 10^4 sequences and a mean library coverage C of >98.5% (data not shown). In total ~22 x 10^4 ZOTUs were determined. A comparison on genus level with published taxa known to contain the *pmo* operon sequences resulted in up to 151 potential methanotrophic ZOTUs, grouping into 15 methanotrophic genera and 5 families (Table S6). The most abundant putative methanotrophic family in amplicon libraries was *Methylacidiphilaceae*, with 71 uncultured ZOTUs followed by *Beijerinckiaceae*. The most abundant genera were *Methylocystis* and the uncultured cluster SH765B-TzT-35 from the *Methylomirabilaceae* family (hereafter referred to as SH765B-TzT-35). In the following, we grouped the ZOTUs belonging to the same genera together in order to simplify the dataset and make changes between the areas better visible.

Most reads affiliating with known methanotrophic taxa reads were found at the Peat site, whereas Forest and Meadow had about half as much reads. In Forest samples, most of such reads were found in the top layer. On the contrary, they increased with depth for the Meadow site until a depth of 8–13 cm and 15–20 cm at the Peat site and decreased afterwards in both cases slightly (Table S6). The top layer at Forest and Meadow sites was with regard to methanotrophic taxa dominated by an uncultured *Methylacidiphilaceae* genus, which relative contribution to all reads decreased with depth (Figure 8). A member of the genus *Methylocystis*, however, dominated the peat site. Its relative abundance first increased to a depth of 20 cm and then abruptly declined at a depth of more than 40 cm. In samples of 40 cm and below SH765B-TzT-35 dominated the methanotrophic community (Figure 8).

In addition to bacterial 16S RNA gene sequencing, we used archaeal primers to identify methanogenic key players. Sequencing resulted in ~9.3 x 10^3 and ~ 1.2 x 10^5 reads per sample with a coverage of >99.9% (data not shown). Overall, 798 ZOTU were identified and a comparison with known methanogenic genera revealed 132 potential methanogenic ZOTU (Table S7). These could be grouped into 11 genera and 9 families (Figure 8). The most abundant genera were *Methanosarcina*, followed by *Methanoregula*, which was almost exclusive present in Peat samples, and third *Methanosaeta*. Together with *Methanobacterium* they account for 96% of methanogenic reads over all samples.

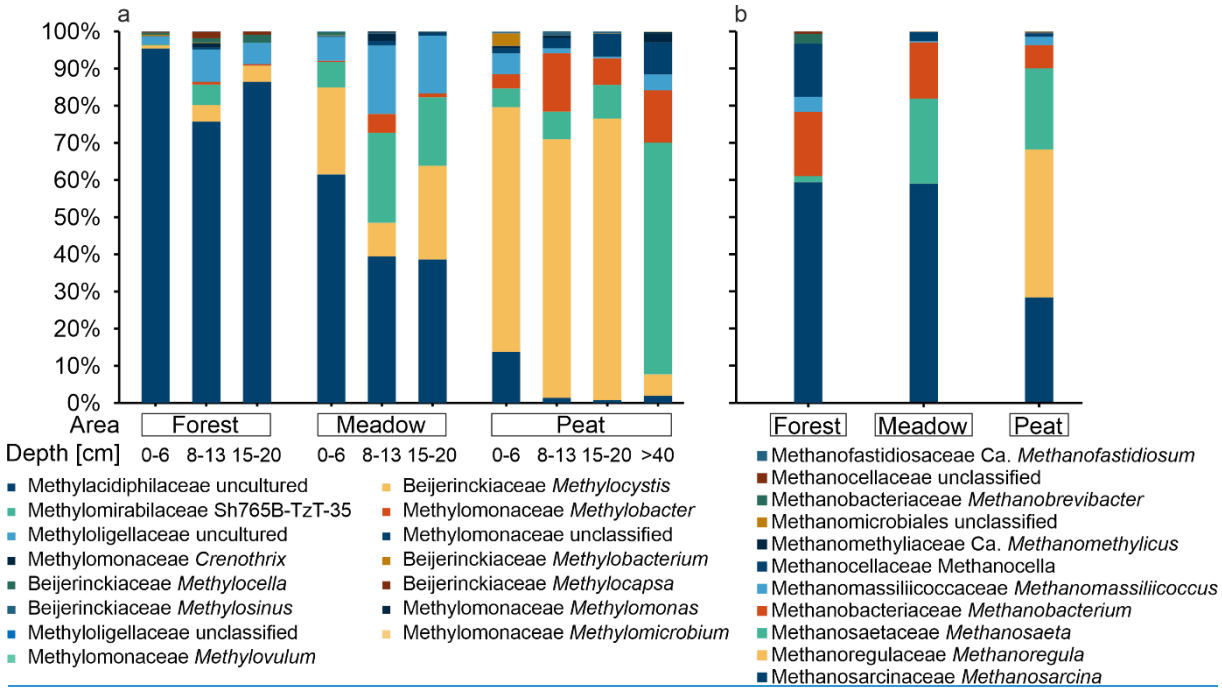

Figure 8: a) Relative abundance of potential methanotrophic genera estimated at three depth intervals detected in the Forest, Meadow, and at four depth intervals in the Peat areas. b) Potential methanogenic genera detected at the three areas Forest, Meadow, and Peat depicted as relative abundance. Reads are displayed as relation to the sum of all reads associated with methanotrophic (a) or methanogenic (b) taxa in the respective sample pool (well and reference sites together).

4 Discussion

4.1 Evaluation of the methodological approach

Abandoned wells in Germany are generally decommissioned and buried (Landesamt für Bergbau, Energie und Geologie (LBEG), 1998). This includes plugging and backfilling of the well, cutting, and removing of the shallow casings, and reconditioning of the area (e.g. for agricultural use). Hence, it is not possible to use the same methods to detect methane from such wells as for wells with visible surface installations, like partly in the US and Canada (Williams et al. 2021, Lebel et al. 2020). As Schout et al. (2019) pointed out, gas leakage of buried wells maybe easily missed by surface measurements alone. In a study with a strategy comparable to ours, Schout et al. (2019) studied potentially leaking (buried) wells in the Netherlands. While different in some aspects, we, however, also used a tandem approach to detect both methane emissions and methane concentrations in the soil gas closer to the buried wells. The combination of both methods is necessary, as high soil gas concentrations did not necessarily correspond to high methane emissions at the same spot (Table S1, S2). Probably due to the high methane oxidation potential of soils in the presence of methanotrophs, as shown previously (Kolb and Horn, 2012; Ho et al., 2019; Guerrero-Cruz et al., 2021). In our case, even measuring points with soil methane concentrations of ~45% of biogenic methane at 20 cm depth, e.g., site WA 264, position 2, were a methane sink at the surface (Table S1, S2). A similar situation was also observed by Schout et al. (2019), who were unable to detect any methane emissions into the atmosphere above a leaking borehole that was detectable at a depth of 2 meters below the soil surface.

Differences between the areas in our study were more pronounced in soil methane concentrations than in methane emissions. These emissions on the other hand, tended to change from source to sink between two measuring points and, thus, on short distances and eventually over time. We therefore conducted a second sampling campaign at the Peat extraction reference site with flux measurements only one meter or less apart to better understand variations on a smaller scale than that usually chosen in our study (10 x 10 m). The transect was chosen to pass through a point with high emissions (Figure 6). The resulting methane fluxes varied more than two orders of magnitude over the distance of less than one meter, whereas CO_2 emissions showed fewer changes and varied in total only by a factor of ~2. This displays the high spatial heterogeneity of the methane emissions and is in agreement with other soil studies (Davidson et al., 2002; Savage et al., 2014; Ambus and Christensen, 1995; Le Mer and Roger, 2001). To address temporal variation, we revisited reference sites in the Forest and Peat up to three times (Figure 1). The overall flux pattern at the Peat site changed from one week to another (Figure S4b, d, f) and fluxes at the same spot differed in part greatly (Table 4), whereas fluxes of two consecutive days differed less. However, soil methane concentration did not vary as much (Table S1). Compared to methane, CO_2 fluxes at the same spots were much more stable and did not show a time dependent variation (Table 4). This temporal data and other data above underline the importance of the use of individual reference measurements. In addition, we propose with regard to our results that a single measurement is not sufficient to evaluate background emissions properly. Both, spatial and temporal variability could be explained by changes in soil compaction (Flechard et al., 2007), differences in moisture content (Basiliko et al., 2007), fluctuating macropores (Schwen et

al., 2015), differing floras (Jentzsch et al., 2024) and microforms (Welpelo et al., 2024) and fauna (Lubbers et al., 2013). Furthermore, occurrence of precipitation and air pressure variations between two consecutive measurements could result in different emission pattern and rates as well (Blagodatsky and Smith, 2012).

Despite the high spatial variation of methane fluxes, we are confident to detect relevant leakage from a well with our strategy due to (1) the combination of flux and soil gas measurements as well as (2) relying on a 17 point grid instead of single measurements. For the grid, we used a distance of 10 m from point to point and ~7 m to the position above the wells at the center of the grid (Figure 2a). These distances are in between the ones used by Sechman (2022) and Schout et al. (2019) who used similar methodical approaches to evaluate the well integrity of buried petroleum and gas wells, respectively.

Considering the main conclusions from our methodological approach, particularly at Peat sites, high methane concentration in addition to methane flux at a well or close by site does not automatically imply a leaking well, as the methane can also origin from shallow methanogenesis. Thus, we determined the methane's isotopic composition $\delta^{13}C\text{-}CH_4$ and $\delta^{2}H\text{-}CH_4$ to distinguish between thermogenic (in our case oil associated) and biogenic methane emissions (Whiticar, 1999; Milkov and Etiope, 2018). Furthermore, we included measurements of all parameters at reference sites to determine the natural biogeochemical background. This approach (see below) helps to get information on whether migration of shallow biogenic methane along the well takes place (e.g., Vielstädte et al., 2015; 2017) or whether natural biogenic methane sources and processes are responsible for methane fluxes.

Table 4: Flux measurements at the Peat reference site (ref.) at the exact same coordinates at different time points.

-	CH_4 [nmol m^{-2} s^{-1}]			CO_2 [µmol m^{-2} s^{-1}]		
-	ref. 3.1	ref. 3.2	ref. 3.3	ref. 3.1	ref. 3.2	ref. 3.3
grid-position	20.04.2022	27.04.2022	28.04.2022	20.04.2022	27.04.2022	28.04.2022
1	273.80	190.43	91.51	3.03	1.66	1.00
2	15.42	381.75	125.38	1.42	2.31	1.70
3	0.21	−0.37	−0.31	1.12	0.76	0.61
4	−0.19	−0.28	−0.26	0.93	0.81	0.54
5	0.02	0.13	0.01	0.44	0.58	0.51
6	31.19	201.39	118.24	1.67	1.87	1.36
7	1.16	55.79	20.91	1.43	2.75	2.53
8	96.14	41.06	15.59	2.72	1.85	1.43
9	32.89	111.38	83.44	1.80	1.38	1.26

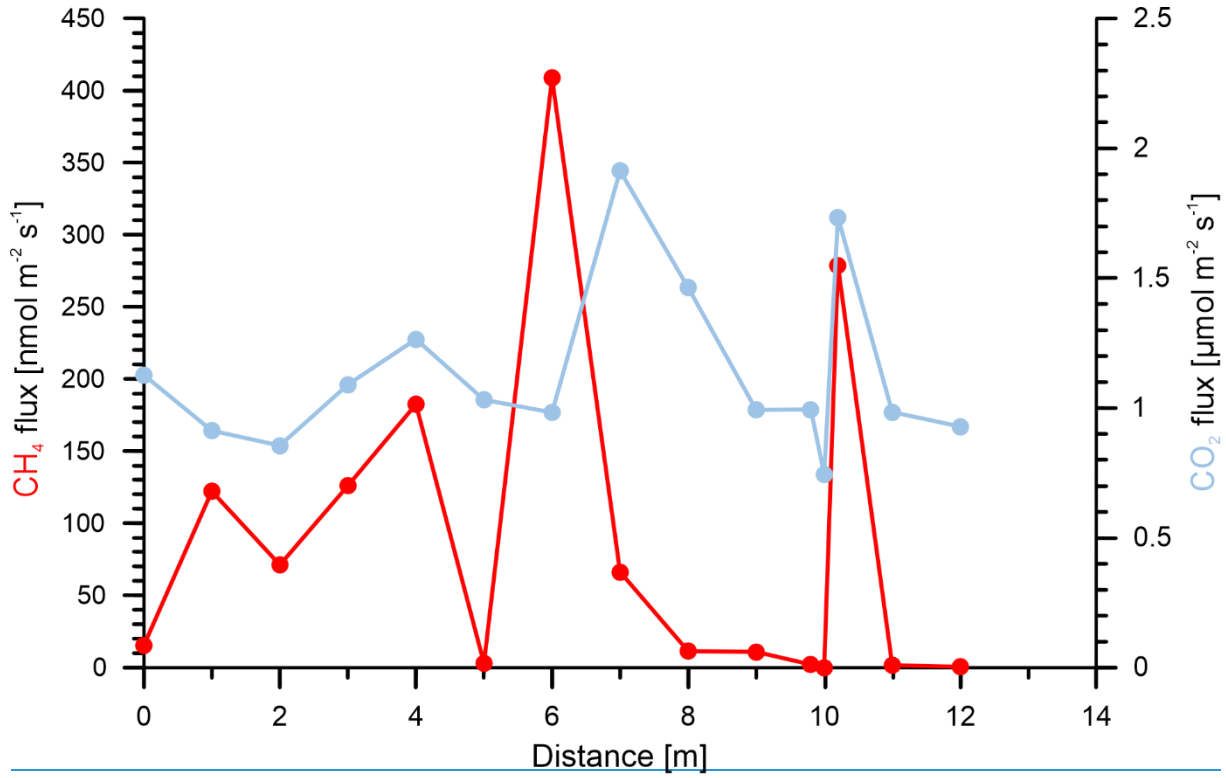

~~**Figure 6:** Methane (blue) and CO_2 (red) fluxes on a meter scale over a 12 m transect at the peat reference site. The fluxes were measured over the course of 3 h. Data is listed in Table S3.~~

4.21 ~~Assessing contribution of abandoned wells to the methane emissions in the studied areas~~Sources of methane in soil and emitted gases

We evaluated methane emission in the described complex and organic rich setting by combining the methane fluxes and soil gas geochemistry. Although these emissions were detected at both the well and the reference sites, it was unclear whether they originated from a leaking well or from methanogenesis. Thus, we determined the isotopic composition of methane (δ^{13}C-CH_4 and δ^{2}H-CH_4) to distinguish between a thermogenic (in our case oil-associated) and a biogenic source of the methane emissions (Schoell 1980, Whiticar, 1999; Milkov and Etiope, 2018). Thermogenic gases, which are produced during the maturation of organic material and which occur in natural gases and oil-associated, are characterized by relatively high δ^{13}C values (> ~–50‰). In combination with δ^{2}H values of the methane, thermogenic origins ~~(natural gas or oil associated)~~ can be well recognized in δ^{13}C/δ^{2}H diagrams (Figure ~~7~~9a). Furthermore, we included measurements of the same parameters at reference sites to determine the natural methane-related biogeochemical background. This approach (see below) helps to get information on whether well-integrity issues, migration of biogenic methane along the well may have taken place (e.g., Vielstädte et al., 2015; 2017) or natural biogenic methane sources and processes in the upper soil are responsible for the methane fluxes.

Using our ~~gas geochemical approach~~emission measurements, we could identify three well sites and their respective reference measurements with net methane emissions (Figure 5, Table ~~1~~2), all of which were located at the Peat site. The first indication that the methane emissions were not oil well-related was that~~,~~ the single peat reference site (measured at three different days) emitted more methane than the corresponding well sites (Table ~~1~~2). ~~All~~ Further, all peat soil gases contained >5% methane with a median of ~35% with no recognizable trend between sites (Table S1). However, ~~The use of the combination of isotope data on carbon and hydrogen in methane is an established method to identify the methane's source (Whiticar, 1999; Schoell, 1980). Thermogenic gases, which are produced during the maturation of organic material and which occur in natural gases and oil associated, are characterized by relatively high $\delta^{13}C$ values (> ~ 50‰). In combination with $\delta^{2}H$ values of the methane, thermogenic origins (natural gas or oil associated) can be well recognized in $\delta^{13}C/\delta^{2}H$ diagrams (Figure 7a). N~~none of the ~~isotopically analyzed~~ methane samples from Steimbke showed an isotopic signature typical for thermogenic methane. Together, ~~T~~this excludes the ~~ebullition~~ leakage of relevant amounts of natural gases from the oil reservoir to the atmosphere or upper soils in Steimbke. ~~Further~~ Finally and supporting this conclusion, oil-associated gases and natural gas contain substantial amounts of ethane and other higher hydrocarbons, which were ~~also not~~only found in trace amounts ~~found~~ in the analyzed gases (Table S1). Both gases (ethane and propane) can be produced in such trace amounts as byproduct during methanogenesis and are typically associated with high amounts of biogenic methane (Schloemer et al. 2018, Oremland et al. 1988).

Methane concentrations were not sufficient for $\delta^{2}H$ analyses in all gas samples, so that the following ~~conclusion~~ does not necessarily hold for low concentrated samples. However, ~~Our~~ our ~~data~~ $\delta^{13}C/\delta^{2}H$ data ~~show~~ indicate that in Steimbke the biogenic methane was formed through ~~other, distinct biogenic, sources for the methane are likely:~~ methanogenesis using acetate (methyl fermentation; acetoclastic) or CO_2-reduction (Figure ~~7b~~9b). ~~While our approach cannot exclude well integrity problems in general, our data argue against methane leakage into the upper soil and/or atmosphere from the reservoir for the studied eight wells in the Steimbke-Nord oil field. Furthermore, the high methane emissions at both, well and reference sites, argues against the migration of shallow biogenic methane along the wells (methane concentrations were not higher in the well grid than in the reference grid samples).~~

Another previously proposed test for well leakage ~~from underground CO_2-storage sites (Romanak et al., 2017; Romanak et al., 2014)~~ focus~~ses~~ed on soil gas composition (Romanak et al., 2017; Romanak et al., 2014). The authors argue that the oxygen and carbon dioxide concentrations in soil gases, driven by normal microbial respiration, should sum-up to around 21%. An excess in CO_2 would hint towards an additional CO_2 source (Romanak et al., 2012). Therefore, they suggest methane from a leaking well, which is oxidized to CO_2, could be such a source or in their investigated case directly leaking CO_2 from a CCS storage site. ~~(Romanak et al., 2012).~~ We observed such enhanced CO_2 concentrations ~~this~~ in the Peats soil gases ~~Forest soil gases~~ (Figure ~~7~~9c). ~~Single~~ Forest measurements and the majority of the Meadow followed, in contrast ~~however~~either~~,~~ a conversion of 1:1 (respiration) or 2:1 oxygen to CO_2, with ~~which~~ the latter correspond~~s~~ing to the stoichiometry of aerobic methane oxidation (Romanak et al., 2012; and references therein). The Peat soil gas compositions spread between both processes and conversions. About half of the samples, however, were enriched in CO_2 (up to 33%). ~~According to Romanak et~~

al. (2012), this indicates an addition of CO_2 or oxidation of exogenous CH_4. The relation of CO_2 to N_2/O_2 is another indication of methane oxidation at the meadow site, however Peat samples indicated excessive CO_2, too (Figure 7e). Following this narrative, only soil gases at the Peat sites were depleted in N_2 (Figure 7f), which indicates leakage or addition of another deeper gas source displacing the atmospheric nitrogen (Romanak et al., 2012). These findings would point to leakage from the abandoned wells at Steimbke, however as we demonstrated above, isotopic compositions as wells as the lack of ethane and propane excludes a thermogenic gas source questioning the possibility to use the model for the interpretation of our study site with a highly active methane cycle. In our view, the drastically increased CO_2 levels in Peat soil gases could be best explained by an extensive degradation of peat by hydrolysis and fermentation to acetate and fatty acids. Those compounds are hereby subsequently converted to methane and CO_2 by acetoclastic methanogenesis with possible contributions of methanogenic conversion of H_2 and CO_2 to methane (e.g. Conrad, 2012). In our view, the drastically increased CO_2 levels in soil gases could be best explained by an extensive microbial degradation of peat via acetate by methanogenesis, which releases methane and CO_2. This is supported by the Peat's high methane and CO_2 concentrations (Figure 97cd). This methane is than oxidized by MOB to CO_2, which further complicates the soil gas interpretation.

While our approach cannot exclude well integrity problems in general, our data argue against methane leakage into the upper soil and/or atmosphere from the reservoir for the studied eight wells in the Steimbke-Nord oil field. Furthermore, the high methane emissions at both, well and reference sites, argues against the migration of shallow biogenic methane along the wells (methane concentrations were not higher in the well grid than in the reference grid samples). A comparison with other reported fluxes underlines that the here determined fluxes (Figure 4) are in the range of natural methane emissions (–2 – 600 nmol m^{-2} s^{-1}, Abdalla et al. 2016) and the lower end of emission rates from abandoned wells (~30 nmol s^{-1} – 800 µmol s^{-1}, Cahill et al. 2023, Williams et al. 2021). Overall, we join previous studies in a call for better surveillance of abandoned wells past abandonment (Cahill et al. 2023, Riddick et al. 2020), more standardization and a comprehensive approach for assessing fugitive gas migration in the field (Samano et al. 2022), and propose the here introduced approach. . In addition, if methane oxidation would be the sole source for the excessive CO_2, this should be visible in the isotopic signature of methane. However, the in the laboratory determined fractionation factor would resulted in the more enriched $\delta^{13}C$ CH_4 and lighter $\delta^{13}C$ CO_2. $\delta^{13}C$ CO_2 was in fact, however, even heavier at the Peat site, which contradicts the interpretation following Romanak et al 2012.

While the soil gas approach by Romanak et al. (2014, 2017) would suggest CO_2 or CH_4 leakage, we were able to disprove this hypothesis in our case. Furthermore, we used this data to look into the apparent differences in methane cycling between the three sites, which will be discussed in the following.

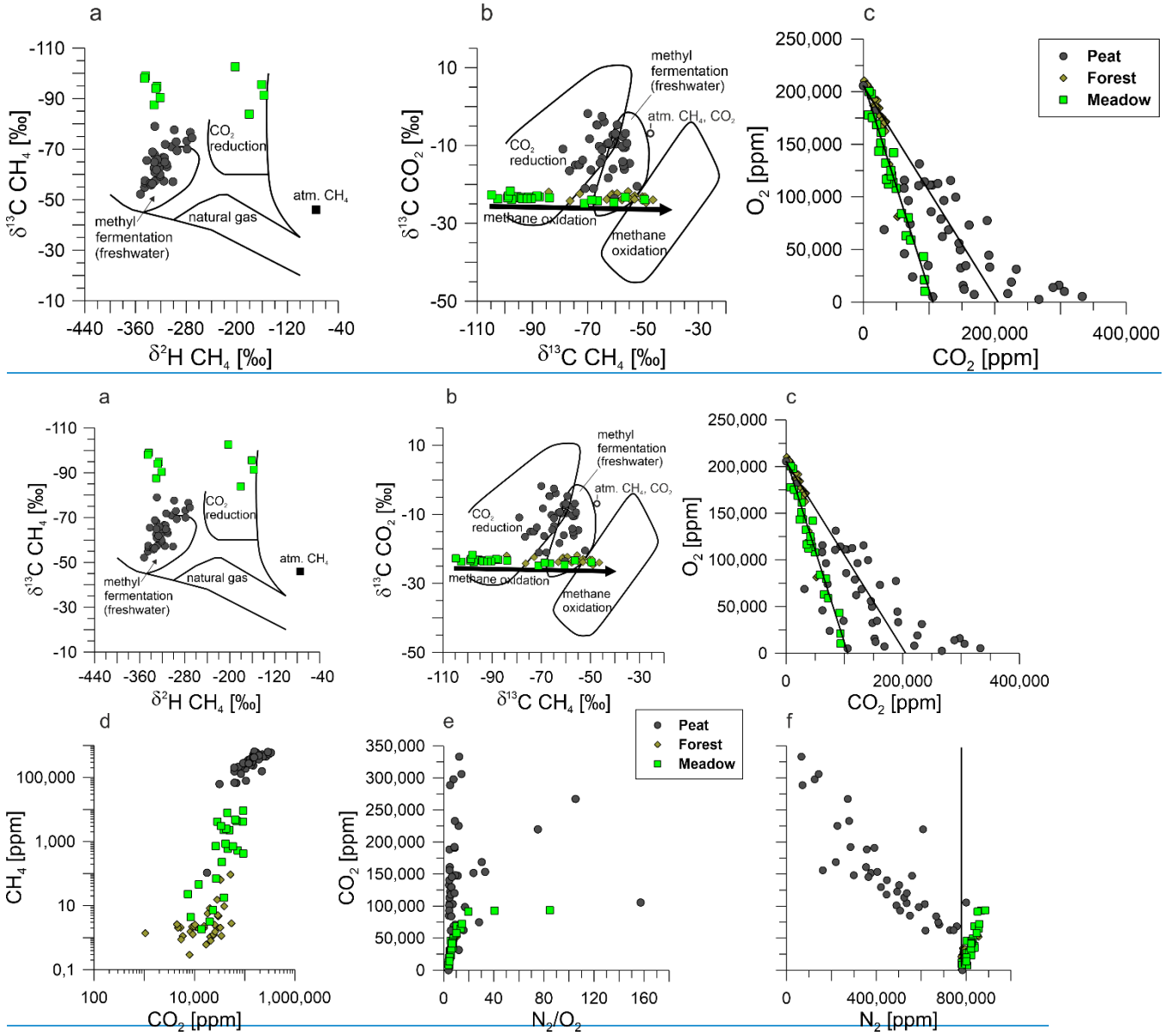

Figure ~~7~~9: Cross-plots of soil gases, namely isotopic composition of a) methane with regard to stable isotopes of carbon and hydrogen as well as ~~d~~b) methane and carbon dioxide to characterize the methane's sources, c) ~~methane~~ oxygen and carbon dioxide ~~(logarithmic scale)~~, ~~d) oxygen and carbon dioxide, e) carbon dioxide and the relation of nitrogen and oxygen, f) carbon dioxide and nitrogen~~ for the three sites Peat (dark grey circles), Forest (~~green~~ brown diamonds), and Meadow ~~(~~(light green squares)~~yellow square)~~. The lines represents in c) left, the consumptions of oxygen via methane oxidation and right for normal soil respiration~~, in f) the atmospheric nitrogen partial pressure~~. Isotopic composition a)~~+~~ and b) after Whiticar (1999). Comparison of ~~carbon dioxide with~~ oxygen and ~~nitrogen~~ CO_2 in panels c)~~–f~~ after Romanak et al. (2012).

4.~~3~~ 2 Natural methane-cycling at the study sites

In the three peat rich surveyed vegetation types in Steimbke, differences in soil gas methane concentrations were more pronounced than in methane emissions. These emissions, however, showed high spatial variations and tended to change from source to sink between two measuring points and, thus, on short distances and eventually over time. We therefore conducted a second sampling campaign at the Peat extraction reference site with flux measurements only one meter or less apart to better understand variations on a smaller scale than the one usually chosen in our study (10 x 10 m). With this new approach, we observed high spatial heterogeneity of the methane emissions (Figure 6), which are in agreement with other soil studies (Davidson et al., 2002; Savage et al., 2014; Ambus and Christensen, 1995; Le Mer and Roger, 2001).

Distinct controls for both, spatial and longer temporal variability could not be resolved in our study but could be explained by changes in soil compaction (Flechard et al., 2007), differences in moisture content (Basiliko et al., 2007), fluctuating macropores (Schwen et al., 2015), differing floras (Jentzsch et al., 2024), microforms (Welpelo et al., 2024) and fauna (Lubbers et al., 2013). Furthermore, precipitation and air pressure variations (i.e., barometric pumping, Forde et al. 2019b) between two consecutive measurements could have affected emission patterns and rates as well (Blagodatsky and Smith, 2012). To address short-term temporal variation, we use the measurements of reference sites in the Peat, which have been visited three times (Figure 3). First on April 20, 2022, and then one week later on two consecutive days (April 27 and 28, 2022). Thereby the overall flux-pattern at the reference site changed from one week to another (Figure S5a, b, c) and fluxes at the same spot differed in part greatly. The fluxes at one point on two consecutive days differed less (Table S2) and the overall pattern remained similar. In contrast, soil methane concentration did not vary as much over time as the respective methane fluxes (Table S1). Compared to methane, CO_2 fluxes at the same spots were much more stable and did not show a time dependent variation (Table S2). This temporal data and the whole data set underline the importance of individual reference measurements and that single measurement points are not sufficient to evaluate background emissions properly.

In natural environments, biogenic methane emissions are the result of the ~~interplay~~ net balance between production and consumption, and the biotic regulation of emissions can occur at the methanogenic and methanotrophic side. Regarding methane production, previous studies discussed ~~these~~ the following possible factors to control methanogenesis in peatlands (1) availability of acetate due to acetate-~~oxidizing~~ producing bacteria outcompeting CO_2-reducing methanogens (Kotsyurbenko, 2005), (2) phenolic compound concentrations~~~~, which might limit peat degradation (Freeman et al., 2001)~~which might limit peat degradation in the Forest and Meadow sites (Freeman et al., 2001)~~, (3) and temperature (Brauer et al., 2006). We ~~consider~~ assume that one or more of these ~~differences~~ controls are also responsible for the presumably different predominating methanogenic pathways indicated by the molecular community analyses and the isotopic compositions of methane in our studied Peat and Meadow areas.~~likely to hold for our studied Peat and Meadow areas with the likely different predominating methanogenic pathways.~~ At all sites both acetoclastic and hydrogenotrophic methanogens were present (Figure 8). ~~Our~~ The genetic ~~analysis~~ analyses ~~of the methanogenic community~~ suggest~~s~~ a higher methanogenic potential at the Peat ~~site~~site, as there were relatively more methanogenic reads found and a higher diversity of methanogens (Figure 8, Table S7). The

acetoclastic methanogenic generas were mostly *Methanosarcina* and *Methanosaeta* ~~are known acetoclastic methanogens~~ whereas the also observed *Methanoregula* and *Methanobacterium* are hydrogenotrophic methanogens (Conrad, 2020). ~~At all sites both acetoclastic and hydrogenotrophic methanogens were present (Figure 5).~~ Soil temperatures were similar at the point of sampling with ~10 ~~°C~~°C, which supported the growth of both acetoclastic and hydrogenotrophic methanogens. ~~The~~ Our isotopic data shown in Fig. ~~7a~~9a, b underline differences between the sites and suggest that methane was produced via ~~two~~ different methanogenic pathways. ~~Namely, t~~The methane at the Peat sites ~~is~~ seems to be mostly derived from acetate ~~whereas~~ in contrast to CO_2 reduction ~~is~~ as the main ~~methanogenesis~~ methanogenic pathway at the Meadow site. This is underlined by the higher mean $\delta^{13}C\text{-}CO_2$ in Peat soil gases (–12‰) compared to soil gases from Meadow and Forest sites (–23.5‰). The first indicate that substantial amounts of CO_2 in Peat soil gases have resulted from fractionating acetoclastic methanogenesis increasing the pool of relatively ^{13}C-enriched CO_2 (Corbett et al. 2012). Methane concentrations in the forest soils were insufficient for $\delta^2H\text{-}CH_4$ measurements. However, the $\delta^{13}C\text{-}CO_2$ and $\delta^{13}C\text{-}CH_4$ data suggest that CO_2 reduction represents the primary methanogenic pathway, with a pronounced isotopic alteration observed in samples with low methane concentrations due to methane oxidation. One explanation for the site dependent difference of the predominant methanogenic pathway could be the differences in peat degradation progression due to the removal of vegetation for peat extraction. The drainage of peatlands is known to lead to decomposition of peat and results in substantial losses of carbon (Couwenberg, 2011). This may in part also explain the higher methane emissions from the active peat extraction site (Peat site) as the drainage of the ~~whole~~ investigate area started already decades ago. However, ~~only recently (starting 2017/18)~~ the peat extraction itself started at this site only recently (2017/18). Thus, we expect that the decomposition of deeper peat layers and the remaining peat intensified after the start of the extraction. Furthermore, about 1 m of peat was already ~~extracted~~ mined from the whole area used for extraction. ~~In addition,~~ This extraction, led to a lowering of the terrain surface (compared to the surroundings) and consequently to a relatively higher water table, which is one of the main factors for higher methane emissions ~~this led as we observed to a higher water table, which is one of the main factor for higher methane emission~~ (Abdalla et al., 2016) as it limits the penetration of oxygen into deeper layers~~as it limits oxygen penetration into deeper layers~~ necessary for methane-oxidizing bacteria (Basiliko et al., 2007). For our gas geochemical study and related sampling strategy, however, a respective in-depth understanding of the drivers for the individual methane-formation pathways was beyond the scope of our study and thus we will in the following focus on the microbial methane filter ~~towards the atmosphere in the following~~.

The observed relatively low potential methane oxidation rates at the Forest sites could result from high affinity methanotrophs, which are specialized to low methane concentrations in well-aerated soils (Bengtson et al., 2009; Kolb, 2009). The very high rates at the Peat site in contrast are an indication of low affinity methanotrophs, which require higher methane concentrations (>100 ppm, Whiticar 2020, and references therein). In combination with these differences in potential methane oxidation rates, ~~O~~our phylogenic data suggests that members of the *Methylacidiphilaceae* family ~~promote~~correspond to ~~atmospheric~~high affinity methane oxidation, whereas *Methylocystis*, *Methylobacter*, and Sh765B-TzT-35 ~~oxidize ascending~~predominate at higher methane concentrations. Kaupper et al. (2021) compared pristine and restored peatlands previously observed a similar shift from *Methylacidiphilaceae* to *Methylocystis* between both settings. So the microbial community at our studied Forest

sites (with peat underneath), which consisted mainly of *Methylacidiphilaceae*, was more similar to that of a pristine peatland than the communities at the other vegetation type settings. The community of the active peat extraction site, which was dominated by *Methylocystis* showed, in contrast, higher similarity to the restored site in Kaupper et al. (2021). This indicates that starting with peat drainage the composition of the methanotrophic community changes but remains active throughout the peat extraction process. Our phylogeny analysis were supported by phospholipid fatty acid (PLFA) analyses of selected samples from the Peat site (Supplements S2), which indicate that the species *Methylocystis heyeri*, a Type II (α-Proteobacteria), was likely involved in methane oxidation at these sites (Figure S2). We also found these PFLA in incubation samples and observed a significant increase after methane addition. ~~In the results we point out, that the Forest sites were characterized as a methane sink with soil methane concentrations at atmospheric levels with one sample at ~100 ppm. In addition, Forest soils showed only minor laboratory methane oxidation rates, one explanation for this could be that the present MOB are specialized for low methane concentrations (Bengtson et al., 2009; Kolb, 2009). The Peat sites on the other hand, showed locally prominent methane fluxes to the atmosphere and methane soil gas concentrations between 1% and 65%. Methane oxidation rates were moderate except for the highest measured rate of 150 µmol s^{-1} g^{-1} (wet soil). The Meadow sites acted as net methane sink, soil methane concentrations were mostly above the atmospheric concentration but below 1%, and oxidation rates were moderate. Methane oxidation rates at both Peat and Meadow sites were, thus, higher than at the Forest site, which coincides with MOB abundance (Table 3). In addition, the higher methane concentrations at the Peat site could enable the growth of low affinity methanotrophs (Christiansen et al., 2014). These methanotrophs require higher methane concentrations (>100 ppm) but are characterized by higher Michaelis–Menten kinetics (Whiticar 2020, and references therein).~~

Especially interesting is that we detected sequences of the genus Sh765B-TzT-35 in deeper and probably anoxic peat layers, which belongs to the family ~~The community analysis revealed a shift from uncultured *Methylacidiphilaceae* at the Forest to members of the *Methylocystis* genus in Peat samples with an additional increase in abundance of Sh765B-TzT-35 (Figure 5). The genus Sh765B-TzT-35 thereby increased with depth and was most abundant in the likely anaerobic layers in the peat at a depth of 40 cm or more. Other members of the~~ *Methylomirabilaceae*. Other members of this family are ~~are~~ known to oxidize methane under anaerobic conditions by internal oxygen production from nitrite reduction to dinitrogen (Ettwig et al., 2010; Versantvoort et al., 2018). Although this internal oxygen production was so far not ~~shown~~ demonstrated for ~~members~~ species of Sh765B-TzT-35, a previous study showed their ability to anaerobically oxidize methane (Nakamura, 2019), which hints towards the same or at least similar mechanisms also for this genus in the studied Peat site.

The discussed methanotrophic community resulted in the highest methane oxidation rates in samples with elevated soil methane concentrations (>4000 ppm), which is in concordance with previous studies (Basiliko et al., 2007; Moore and Dalva, 1997). It was recently shown, that in addition to substrate availability (here methane concentration), the methanotrophic community can be influenced by physico-chemical parameters and land use (Kaupper et al., 2022 and references therein). Kaupper et al. (2022) showed that the environmental parameters, total C and N content, and electrical conductivity, indicative of salinity, affected the active bacterial community. This suggests that the methanotrophic communities can adapt to different

methane regimes and, as speculation, could mitigate an occurring potential methane leakage from an underlying abandoned well over time. ~~Our phylogenic data suggests that members of the *Methylacidiphilaceae* family promote atmospheric methane oxidation whereas *Methylocystis*, *Methylobacter*, and Sh765B-TzT-35 oxidize ascending methane.~~ ~~Kaupper et al. (2021) who compared pristine and restored peatlands previously observed a similar shift from *Methylacidiphilaceae* to *Methylocystis*. Simplified, one can content that the microbial community at our studied Forest site was similar to that of a pristine peatland. The active peat extraction site, on the other hand, showed similarity to the restored site in Kaupper et al. (2021). This indicates that starting with peat drainage the methanotrophic community shifts but remains active throughout the extraction process. However, it takes the microbial community decades to restore pristine like diversity and complexity (Kaupper et al., 2021). Geochemical and molecular microbial work also underline the differences between all sites. Our phylogeny analysis were supported by phospholipid fatty acid (PLFA) analyses of selected samples from the Peat site, which indicate that *Methylocystis heyeri*, a Type II (α Proteobacteria), was likely involved in methane oxidation at these sites (Figure S1). We also found these PFLA in incubation samples and observed a significant increase after methane addition. Methane oxidation rates were highest in samples with elevated soil methane concentrations (>4000 ppm), which is in concordance with previous studies (Basiliko et al., 2007; Moore and Dalva, 1997). It was previously shown, that in addition to substrate availability (here methane concentration), the methanotrophic community can be influenced by physico-chemical parameters and land use (Kaupper et al., 2022) references therein. Kaupper et al. (2022) showed that the environmental parameters, total C and N content, and electrical conductivity, indicative of salinity, affected the active bacterial community. This suggests that the methanotrophic communities can adapt to different methane regimes and, as speculation, could mitigate a potential leakage over time.~~

Converting our values for mean methane emissions to enable the comparison with literature data, we observed an emission rate of ~23 g m^{-2} yr^{-1} for the Peat sites. These numbers are in our case without emissions from ditches, which Sundh et al. (2000) showed can be substantial. An in-depth study on the influence of vegetation on methane emission conducted by Welpelo et al. (2024) at a rewetted peat site about 3 km north-west from our study area, estimated yearly emission between 7.1 and 36.1 g m^{-2} $year^{-1}$. As our field campaign was conducted in April 2022, and we observed comparable methane emissions to their combination of measurement and modeling for the same season, our ~~yearly~~ estimation seems plausible, although, the Peat's groundwater table was comparably lower. The emissions at the Peat extraction site's (our study) were about twice (Strack et al., 2016) to more than hundredfold (Wilson et al., 2016) higher than from pristine peat sites and about tenfold higher than from a restored peatland (Strack et al., 2014). ~~Since~~ The carbon dioxide emissions (Table S2) from the Peat sites were ~~not elevated~~similar to another unrestored peat extraction site (Strack et al. 2014). ~~, one can assume that the Peat site acted emission wise more like a wetland without vegetation than a drained peatland.~~ In addition, it is possible that the progressed peat extraction provided a different type and quality of organic precursor substrates than the Forest and Meadow sites as suggested from and observed in other peat sites (Alstad and Whiticar, 2011). Our data suggest that active peat extraction sites can be significant methane sources and that these areas do not necessarily emit less methane than rewetted ones as stated in literature (Welpelo et al., 2024; Bieniada and Strack, 2021; Rankin et al., 2018; Abdalla et al., 2016) ~~and that these areas can be significant methane sources~~.

~~Overall, we conclude that there is no connection between the methane emissions detected and the abandoned wells investigated. Furthermore, the factors discussed above suggest that the level of disturbance can be considered as the major driving force for the here shown methane emissions. Thus, the anthropogenic influences play a key role for methane formation and emission in such altered ecosystems.~~

4.3 Extent of natural microbial mitigation of potential subsurface leakage

Our data, which is in line with another study on buried abandoned wells in the Netherlands (Schout et al. 2019), suggests that relying only on methane emission measurements to detect well leakage can be associated with the risk of missing integrity-compromised wells. In our case, at some measuring points soil methane concentrations reached ~45% of biogenic methane at 20 cm depth, e.g., site R-WA 264, position 2, but the soils still acted as a methane sink at the surface (–1.2 nmol m^{-2} s^{-1}, Table S1, S2). This is probably due to the high methane oxidation potential in these soils due to the presence of a large population of methanotrophs (Figure 8, Table S6), which has also be reported previously (Kolb and Horn, 2012; Ho et al., 2019; Guerrero-Cruz et al., 2021).

It remains unclear to what extent natural microbial oxidation capacities for methane could degrade upward migrating methane in the soil in the event of a broken gas or oil well. This will most likely be less efficient at the beginning of a leakage, but might rapidly increase due to the adaptation of the respective microbial communities in the affected soil layers. However, such processes could be highly relevant for Germany, as 15% of abandoned wells in Germany are located in areas with highly organic-rich soils such as peat (mostly in Northern Germany). These areas most likely already contain a microbial community preadapted due to the naturally elevated methane concentrations. In a recent study, Schout et al. (2019) observed such a situation, as they were unable to detect any methane emissions into the atmosphere above a leaking borehole, but could show high methane fluxes after removing the top 2 m of the soil and, thus, the microbial methane filter. This is also in-line with a study by Cahill et al. (2023), who found that 5 out of 10 surveyed wells (9 unconventional) in Canada were leaking fugitive methane, however only two showed direct methane emission (up to 3 x 10^3 nmol m^{-2} s^{-1}) whereas the other were emitting elevated levels of CO_2 (up to 15 µmol m^{-2} s^{-1}). These CO_2 fluxes were interpreted to result from enhanced bacterial methane oxidation mitigating the fugitive methane release from leaking abandoned wells by natural soils (here with a lower organic carbon content) and lowered the total greenhouse gas emission substantially. However, in addition to indirect indications such as $\delta^{13}C$-CO_2 values (Cahill et al. 2023), our study demonstrated that it is advantageous to also determine methane oxidation rates. Here, we measured high methane oxidation capacities of (wet) peat samples in our lab of up to ~14,000 nmol CH_4 0.2 m^{-3} s^{-1} (= 0.8 g 0.2 m^{-3} h^{-1}, Table 3). To put this in perspective, methane leakage rates from plugged wells in two regions in Canada ranged between 0.04 to 1 g CH_4 $well^{-1}$ h^{-1} (Bowman et al., 2023) and up to ~0.2 g $well^{-1}$ h^{-1} from unconventional plugged wells (Cahill et al. 2023) are similar in ranges. Further research is required to examine the activity and precise functioning of this microbial filter, with particular attention paid to the influence of seasonality (i.e., temperature).

5 Conclusion

In the worldwide efforts to mitigate anthropogenic methane emissions, which are a key factor for climate change, a comprehensive approach is needed. One of these sectors is the oil & gas industry and although research targeting abandoned wells developed momentum, financial resources to backfill additional wells are limited (Raimi et al., 2021) and progression advances slowly. Especially orphaned and abandoned wells in the USA and Canada are an active area of research as they are mostly not properly decommissioned and thus prone to leakage. In several studies, high methane emissions (several tons per year) from such wells were observed (i.e., Boutot et al., 2022; Bowman et al., 2023; Hac{El Hachem, 2022 #119}hem & Kang, 2023). Plugged and buried abandoned wells on the other hand were so far poorly studied, and data on location and history of these wells is often limited. In this study, we demonstrate a methodological approach to survey such cut and buried abandoned wells to unravel the methane emissions origin in a complex peat rich setting with a distinctive methane cycle containing several abandoned wells. The approach combined methane flux measurements spanning an area of 30 x 30 m around the well location and a 20 x 20 reference area with the characterization of soil gas samples, and determination of the methane's isotopic composition, respectively. In total, we sampled eight well site, out of which three showed net methane emissions to the atmosphere, all located in an active peat extraction site. However, similar methane abundances at related reference site as well as soil gas and isotopic composition revealed a biogenic origin, thus confirming that the surveilled abandoned wells did not emit methane to the upper soil and atmosphere originating. The methane emission patterns exhibited a substantial spatial variability. Methane concentrations in the soil gas on the other hand were much more homogenous. Subsequent microbial analyses showed substantial methane oxidation capacities at the Peat site. In combination with phylogenetic data, we suggest that established methanotrophic communities act as an efficient aerobic methane filter and may pose as a potential barrier for small leakages. However, further research is necessary to determine their mitigation potential and respective work is ongoing. It remains unclear to what extent natural microbial oxidation capacities for methane could degrade methane in the ground from theoretical leaks in the event of a broken well. However, such processes could be highly relevant for Germany, as 15 % of abandoned wells in Germany are located in areas with highly organic rich soils such as peat (mostly in Northern Germany). Furthermore, our data showed mean methanotrophy capacities of (wet) peat samples in our lab up to ~14,000 nmol CH_4 0.2 m^{-3} s^{-1} (Table 3; = 0.8 g 0.2 m^{-3} h^{-1}). To put this in perspective, methane leakage rates from plugged wells in two regions in Canada ranged between 0.04 to 1 g CH_4 $well^{-1}$ h^{-1} (Bowman et al., 2023).

Exclusively emission based approaches, such as the use of emission chambers, survey cars, specialized cameras etc., are not suited for buried wells as they would be susceptible to the misinterpretation of natural methane emissions. For a conclusive surveillance of cut and buried abandoned wells, the here presented multilayered strategy determining methane emissions, soil

~~gas composition and isotopic signatures, ideally together with microbiological techniques in comparison with carefully selected reference sites is necessary.~~

While it is well known that abandoned oil and gas wells can have integrity issues, respective knowledge particularly on the 20,000 cut and buried wells in Germany, is lacking. Here we provide with our multi-methodological approach first data on potential methane fluxes from abandoned oil wells to the atmosphere. We combined emission data (positive and negative) at wells and reference areas with gas geochemical characterization of soil gas samples to investigate eight wells in a peat rich setting with three different land use types (Forest, Meadow, Peat extraction).

The Peat extraction site was the only one, which emitted substantial amounts of methane. However, in general no difference in surface methane emission rates between well and reference sites independent of site characteristics (active peat mining, drained peat vegetated with birch trees or grassland) were observed. With respect to soil gases, the three areas showed highly variable but spatially correlating (i.e. area specific) methane concentrations concurring with CO_2 concentrations. The in-depth gas and isotope geochemical analysis revealed biogenic methane as source for the net emissions at the open peat site (methyl fermentation) and the meadow (CO_2 reduction pathway with partial methane oxidation). These findings and the absence of higher hydrocarbons excludes thermogenic gas emissions from the plugged wells. Overall, we conclude that there is no connection between the methane emissions detected and the abandoned wells investigated. Furthermore, the factors discussed above suggest that the level of disturbance can be considered as the major driving force for the here shown methane emissions. Thus, the anthropogenic influences play a key-role for methane formation and emission in such altered ecosystems.

Furthermore, the laboratory methane oxidation rates derived from our incubated peat samples demonstrated the capacity to counterbalance reported leakage rates for buried abandoned wells in other regions. The activity of such a microbial methane filter poses the risk for false negative leakage classification. Overall the observed methanotrophy could be highly relevant for Germany as 15% of our cut and buried wells are located in areas with very organic-rich soils. However, for a comprehensive evaluation of the situation of abandoned wells in Germany further investigations are needed. Therefore, additional sampling at different sites (oil/gas wells of different age and deconstruction histories) in Northern Germany with the here introduced methodology are under way and we will evaluate the natural mitigation potential for different soil types and land uses.

In conclusion, exclusively using emission-based approaches are not suited for integrity failure assessments of buried wells as these would be susceptible to misinterpretations. We highly recommend a holistic approach for surveillance including the determination of methane emission, soil gas composition and isotopic signatures at and in the vicinity of well sites against the background of a carefully selected reference site.~~.~~

6 Acknowledgement

We thank Daniela Zoch, Daniela Graskamp, Thilo Falkenberg, Laurin Rösler, Lukas Heine, Nicole Becker, Alana Zimmer, Georg Scheeder, Dietmar Laszinski, and Christian Seeger for their help in the field and laboratory. Furthermore, we thank Christian Ostertag-Henning for fruitful scientific discussions and the local peat extraction company for repeated access to the study site. The BGR internal funding through project A-0202019.A and DFG grant HO 6234/1-2 made this study possible.

7 Data availability

Measured and derived data supporting the findings of this study are available in the supplementary data sheet.

8 Author contributions

M.B., S.S., S.F.A.J., and M.K. conceived and designed the experiments. S.F.A.J., S.S., M.B., M.K. conducted the fieldwork and performed the experiments. S.F.A.J. and T.H. performed qPCR and processed the data. Main data interpretation was performed by S.F.A.J. in cooperation with the co-authors. S.F.A.J. wrote the main manuscript text with input from M.B., S.S., M.K., T.H., ~~M.A.H~~and M.A.H. All authors read and approved the final version of the manuscript.

9 Competing interests

The authors declare no competing interests.

7 References

Abdalla, M., Hastings, A., Truu, J., Espenberg, M., Mander, U., and Smith, P.: Emissions of methane from northern peatlands: a review of management impacts and implications for future management options, Ecol Evol, 6, 7080-7102, https://doi.org/10.1002/ece3.2469, 2016.

Agerton, M., Narra, S., Snyder, B., and Upton, G. B.: Financial liabilities and environmental implications of unplugged wells for the Gulf of Mexico and coastal waters, Nature Energy, 8, 536-547, https://doi.org/10.1038/s41560-023-01248-1, 2023.

Alstad, K. P. and Whiticar, M. J.: Carbon and hydrogen isotope ratio characterization of methane dynamics for Fluxnet Peatland Ecosystems, Org Geochem, 42, 548-558, https://doi.org/10.1016/j.orggeochem.2011.03.004, 2011.

Ambus, P. and Christensen, S.: Spatial and Seasonal Nitrous Oxide and Methane Fluxes in Danish Forest-, Grassland-, and Agroecosystems, J Environ Qual, 24, 993-1001, https://doi.org/10.2134/jeq1995.00472425002400050031x, 1995.

Basiliko, N., Blodau, C., Roehm, C., Bengtson, P., and Moore, T. R.: Regulation of Decomposition and Methane Dynamics across Natural, Commercially Mined, and Restored Northern Peatlands, Ecosystems, 10, 1148-1165, https://doi.org/10.1007/s10021-007-9083-2, 2007.

Belyea, L. R.: Nonlinear Dynamics of Peatlands and Potential Feedbacks on the Climate System, in: Carbon Cycling in Northern Peatlands, Geoph Mono, 5-18, https://doi.org/10.1029/2008gm000829, 2013.

Bengtson, P., Basiliko, N., Dumont, M. G., Hills, M., Murrell, J. C., Roy, R., and Grayston, S. J.: Links between methanotroph community composition and CH_4 oxidation in a pine forest soil, FEMS Microbiol Ecol, 70, 356-366, https://doi.org/10.1111/j.1574-6941.2009.00751.x, 2009.

Bieniada, A. and Strack, M.: Steady and ebullitive methane fluxes from active, restored and unrestored horticultural peatlands, Ecol Eng, 169, https://doi.org/10.1016/j.ecoleng.2021.106324, 2021.

Blagodatsky, S. and Smith, P.: Soil physics meets soil biology: Towards better mechanistic prediction of greenhouse gas emissions from soil, Soil Biol Biochem, 47, 78-92, https://doi.org/10.1016/j.soilbio.2011.12.015, 2012.

Boutot, J., Peltz, A. S., McVay, R., and Kang, M.: Documented Orphaned Oil and Gas Wells Across the United States, Environ Sci Technol, 56, 14228-14236, https://doi.org/10.1021/acs.est.2c03268, 2022.

Bowman, L. V., El Hachem, K., and Kang, M.: Methane Emissions from Abandoned Oil and Gas Wells in Alberta and Saskatchewan, Canada: The Role of Surface Casing Vent Flows, Environ Sci Technol, https://doi.org/10.1021/acs.est.3c06946, 2023.

Brauer, S. L., Cadillo-Quiroz, H., Yashiro, E., Yavitt, J. B., and Zinder, S. H.: Isolation of a novel acidiphilic methanogen from an acidic peat bog, Nature, 442, 192-194, https://doi.org/10.1038/nature04810, 2006.

Cahill, A. G., Joukar, M., Sefat, M., and van Geloven, C.: Evaluating Methane Emissions From Decommissioned Unconventional Petroleum Wells in British Columbia, Canada, Geophys Res Lett, 50, https://doi.org10.1029/2023gl106496, 2023.

Caporaso, J. G., Lauber, C. L., Walters, W. A., Berg-Lyons, D., Lozupone, C. A., Turnbaugh, P. J., Fierer, N., and Knight, R.: Global patterns of 16S rRNA diversity at a depth of millions of sequences per sample, Proc Natl Acad Sci U S A, 108 Suppl 1, 4516-4522, https://doi.org/10.1073/pnas.1000080107, 2011.

~~Christiansen, J. R., Romero, A. J. B., Jørgensen, N. O. G., Glaring, M. A., Jørgensen, C. J., Berg, L. K., and Elberling, B.: Methane fluxes and the functional groups of methanotrophs and methanogens in a young Arctic landscape on Disko Island, West Greenland, Biogeochemistry, 122, 15-33, https://doi.org/10.1007/s10533-014-0026-7, 2014.~~

Cleary, J., Roulet, N. T., and Moore, T. R.: Greenhouse gas emissions from Canadian peat extraction, 1990-2000: a life-cycle analysis, Ambio, 34, 456-461, https://doi.org/10.1579/0044-7447-34.6.456, 2005.

Conrad, R.: Importance of hydrogenotrophic, aceticlastic and methylotrophic methanogenesis for methane production in terrestrial, aquatic and other anoxic environments: A mini review, Pedosphere, 30, 25-39, https://doi.org/10.1016/s1002-0160(18)60052-9, 2020.

Coplen, T. B.: Guidelines and recommended terms for expression of stable-isotope-ratio and gas-ratio measurement results, Rapid Commun Mass Spectrom, 25, 2538-2560, https://doi.org/10.1002/rcm.5129, 2011.

Corbett, J. E., Tfaily, M. M., Burdige, D. J., Cooper, W. T., Glaser, P. H., and Chanton, J. P.: Partitioning pathways of CO2 production in peatlands with stable carbon isotopes, Biogeochemistry, 114, 327-340, https://doi.org/10.1007/s10533-012-9813-1, 2012.

Costello, A. M. and Lidstrom, M. E.: Molecular characterization of functional and phylogenetic genes from natural populations of methanotrophs in lake sediments, Appl Environ Microbiol, 65, 5066-5074, https://doi.org/10.1128/AEM.65.11.5066-5074.1999, 1999.

Couwenberg, J.: Greenhouse gas emissions from managed peat soils: is the IPCC reporting guidance realistic?, Mires Peat, 8, 2011.

Davies, R. J., Almond, S., Ward, R. S., Jackson, R. B., Adams, C., Worrall, F., Herringshaw, L. G., Gluyas, J. G., and Whitehead, M. A.: Oil and gas wells and their integrity: Implications for shale and unconventional resource exploitation, Mar Pet Geol, 56, 239-254, https://doi.org/10.1016/j.marpetgeo.2014.03.001, 2014

Davidson, E. A., Savage, K., Verchot, L. V., and Navarro, R.: Minimizing artifacts and biases in chamber-based measurements of soil respiration, Agr Forest Meteorol, 113, 21-37, https://doi.org/10.1016/s0168-1923(02)00100-4, 2002.

Dennis, L. E., Richardson, S. J., Miles, N., Woda, J., Brantley, S. L., and Davis, K. J.: Measurements of Atmospheric Methane Emissions from Stray Gas Migration: A Case Study from the Marcellus Shale, ACS Earth Space Chem, 6, 909-919, https://doi.org/10.1021/acsearthspacechem.1c00312, 2022.

Dohrmann, A. B. and Krüger, M.: Microbial H_2 Consumption by a Formation Fluid from a Natural Gas Field at High-Pressure Conditions Relevant for Underground H_2 Storage, Environ Sci Technol, 57, 1092-1102, https://doi.org/10.1021/acs.est.2c07303, 2023.

Drake, H. L., Horn, M. A., and Wust, P. K.: Intermediary ecosystem metabolism as a main driver of methanogenesis in acidic wetland soil, Environ Microbiol Rep, 1, 307-318, https://doi.org/10.1111/j.1758-2229.2009.00050.x, 2009.

Edgar, R. C.: Search and clustering orders of magnitude faster than BLAST, Bioinformatics, 26, 2460-2461, https://doi.org/10.1093/bioinformatics/btq461, 2010.

Edgar, R. C.: UNOISE2: improved error-correction for Illumina 16S and ITS amplicon sequencing., bioRxiv [preprint], https://doi.org/10.1101/081257, 2016.

El Hachem, K. and Kang, M.: Methane and hydrogen sulfide emissions from abandoned, active, and marginally producing oil and gas wells in Ontario, Canada, Sci Total Environ, 823, 153491, https://doi.org/10.1016/j.scitotenv.2022.153491, 2022.

Ettwig, K. F., Butler, M. K., Le Paslier, D., Pelletier, E., Mangenot, S., Kuypers, M. M., Schreiber, F., Dutilh, B. E., Zedelius, J., de Beer, D., Gloerich, J., Wessels, H. J., van Alen, T., Luesken, F., Wu, M. L., van de Pas-Schoonen, K. T., Op den Camp, H. J., Janssen-Megens, E. M., Francoijs, K. J., Stunnenberg, H., Weissenbach, J., Jetten, M. S., and Strous, M.: Nitrite-driven anaerobic methane oxidation by oxygenic bacteria, Nature, 464, 543-548, https://doi.org/10.1038/nature08883, 2010.

Feisthauer, S., Vogt, C., Modrzynski, J., Szlenkier, M., Krüger, M., Siegert, M., and Richnow, H.-H.: Different types of methane monooxygenases produce similar carbon and hydrogen isotope fractionation patterns during methane oxidation, Geochim Cosmochim Ac, 75, 1173-1184, https://doi.org/10.1016/j.gca.2010.12.006, 2011.

Flechard, C. R., Ambus, P., Skiba, U., Rees, R. M., Hensen, A., van Amstel, A., Dasselaar, A. v. d. P.-v., Soussana, J. F., Jones, M., Clifton-Brown, J., Raschi, A., Horvath, L., Neftel, A., Jocher, M., Ammann, C., Leifeld, J., Fuhrer, J., Calanca, P., Thalman, E., Pilegaard, K., Di Marco, C., Campbell, C., Nemitz, E., Hargreaves, K. J., Levy, P. E., Ball, B. C., Jones, S. K., van de Bulk, W. C. M., Groot, T., Blom, M., Domingues, R., Kasper, G., Allard, V., Ceschia, E., Cellier, P., Laville, P., Henault, C., Bizouard, F., Abdalla, M., Williams, M., Baronti, S., Berretti, F., and Grosz, B.: Effects of climate and management intensity on nitrous oxide emissions in grassland systems across Europe, Agric Ecosyst Environ, 121, 135-152, https://doi.org/10.1016/j.agee.2006.12.024, 2007.

Forde, O. N., Mayer, K. U., and Hunkeler, D.: Identification, spatial extent and distribution of fugitive gas migration on the well pad scale, Sci Total Environ, 652, 356-366, https://doi.org/10.1016/j.scitotenv.2018.10.217, 2019a.

Forde, O. N., Cahill, A. G., Beckie, R. D., and Mayer, K. U.: Barometric-pumping controls fugitive gas emissions from a vadose zone natural gas release, Sci Rep, 9, 14080, https://doi.org/10.1038/s41598-019-50426-3, 2019b.

Forde, O. N., Cahill, A. G., Mayer, B., Beckie, R. D., and Mayer, K. U.: Fugitive Gas Migration in the Vadose Zone at an Experimental Field Site in the Montney Shale Gas Region, Geophys Res Lett, 49, https://doi.org/10.1029/2022gl098762, 2022.

Freeman, C., Ostle, N., and Kang, H.: An enzymic 'latch' on a global carbon store, Nature, 409, 149, https://doi.org/10.1038/35051650, 2001.

Frolking, S., Roulet, N., and Fuglestvedt, J.: How northern peatlands influence the Earth's radiative budget: Sustained methane emission versus sustained carbon sequestration, J Geophys Res Biogeosci, 111, https://doi.org/10.1029/2005jg000091, 2006.

Gantner, S., Andersson, A. F., Alonso-Saez, L., and Bertilsson, S.: Novel primers for 16S rRNA-based archaeal community analyses in environmental samples, J Microbiol Meth, 84, 12-18, https://doi.org/10.1016/j.mimet.2010.10.001, 2011.

Guerrero-Cruz, S., Vaksmaa, A., Horn, M. A., Niemann, H., Pijuan, M., and Ho, A.: Methanotrophs: Discoveries, Environmental Relevance, and a Perspective on Current and Future Applications, Front Microbiol, 12, 678057, https://doi.org/10.3389/fmicb.2021.678057, 2021.

Hedrich, S., Guezennec, A. G., Charron, M., Schippers, A., and Joulian, C.: Quantitative Monitoring of Microbial Species during Bioleaching of a Copper Concentrate, Front Microbiol, 7, 2044, https://doi.org/10.3389/fmicb.2016.02044, 2016.

Ho, A., Kwon, M., Horn, M. A., and Yoon, S.: Environmental Applications of Methanotrophs, in: Methanotrophs, Micro Mono, 231-255, https://doi.org/10.1007/978-3-030-23261-0_8, 2019.

IEA: Global Methane Tracker 2024, IEA, Paris https://www.iea.org/reports/global-methane-tracker-2024, 2024 BY 4.0

Jentzsch, K., Männistö, E., Marushchak, M. E., Korrensalo, A., van Delden, L., Tuittila, E.-S., Knoblauch, C., and Treat, C. C.: Seasonal controls on methane flux components in a boreal peatland - combining plant removal and stable isotope analyses, EGUsphere [preprint], https://doi.org/10.5194/egusphere-2023-3098, 2024.

Kang, M., Brandt, A. R., Zheng, Z., Boutot, J., Yung, C., Peltz, A. S., and Jackson, R. B.: Orphaned oil and gas well stimulus—Maximizing economic and environmental benefits, Elem Sci Anth, 9, https://doi.org/10.1525/elementa.2020.20.00161, 2021

Kartenserver, N.: Oil & Gas fields - Landesamt für Bergbau, Energie und Geologie (LBEG), Hannover. [dataset], 2014a.

Kartenserver, N.: Network Hydrocarbon-Geology (KW-Verbund). - Landesamt für Bergbau, Energie und Geologie (LBEG), Hannover. [dataset], 2014b.

Kaupper, T., Mendes, L. W., Harnisz, M., Krause, S. M. B., Horn, M. A., and Ho, A.: Recovery in methanotrophic activity does not reflect on the methane-driven interaction network after peat mining, Appl Environ Microbiol, 87, https://doi.org/10.1128/AEM.02355-20, 2021.

Kaupper, T., Mendes, L. W., Poehlein, A., Frohloff, D., Rohrbach, S., Horn, M. A., and Ho, A.: The methane-driven interaction network in terrestrial methane hotspots, Environ Microbiome, 17, 15, https://doi.org/10.1186/s40793-022-00409-1, 2022.

Knief, C.: Diversity and Habitat Preferences of Cultivated and Uncultivated Aerobic Methanotrophic Bacteria Evaluated Based on *pmoA* as Molecular Marker, Front Microbiol, 6, 1346, https://doi.org/10.3389/fmicb.2015.01346, 2015.

Knief, C.: Diversity of Methane Cycling Microorganisms in Soils and Their Relation to Oxygen, Curr Issues Mol Biol, 33, 23-56, https://doi.org/10.21775/cimb.033.023, 2019.

Kolb, S.: The quest for atmospheric methane oxidizers in forest soils, Environ Microbiol Rep, 1, 336-346, https://doi.org/10.1111/j.1758-2229.2009.00047.x, 2009.

Kolb, S. and Horn, M. A.: Microbial CH_4 and N_2O Consumption in Acidic Wetlands, Front Microbiol, 3, 78, https://doi.org/10.3389/fmicb.2012.00078, 2012.

Kotsyurbenko, O. R.: Trophic interactions in the methanogenic microbial community of low-temperature terrestrial ecosystems, FEMS Microbiol Ecol, 53, 3-13, https://doi.org/10.1016/j.femsec.2004.12.009, 2005.

Lai, D. Y. F.: Methane Dynamics in Northern Peatlands: A Review, Pedosphere, 19, 409-421, https://doi.org/10.1016/s1002-0160(09)00003-4, 2009.

Laine, J., Minkkinen, K., and Trettin, C.: Direct Human Impacts on the Peatland Carbon Sink, in: Carbon Cycling in Northern Peatlands, Geoph Mono, 71-78, https://doi.org/10.1029/2008gm000808, 2013.

Landesamt für Bergbau, Energie und Geologie (LBEG): RV: 4.25 Richtlinien über das Verfüllen auflässiger Bohrungen, 1998.

Le Mer, J. and Roger, P.: Production, oxidation, emission and consumption of methane by soils: A review, Eur J Soil Biol, 37, 25-50, https://doi.org/10.1016/s1164-5563(01)01067-6, 2001.
Lebel, E. D., Lu, H. S., Vielstadte, L., Kang, M., Banner, P., Fischer, M. L., and Jackson, R. B.: Methane Emissions from Abandoned Oil and Gas Wells in California, Environ Sci Technol, 54, 14617-14626, https://doi.org/10.1021/acs.est.0c05279, 2020.
Liu, Y. and Whitman, W. B.: Metabolic, phylogenetic, and ecological diversity of the methanogenic archaea, Ann N Y Acad Sci, 1125, 171-189, https://doi.org/10.1196/annals.1419.019, 2008.
Lubbers, I. M., van Groenigen, K. J., Fonte, S. J., Six, J., Brussaard, L., and van Groenigen, J. W.: Greenhouse-gas emissions from soils increased by earthworms, Nat Clim Change, 3, 187-194, https://doi.org/10.1038/nclimate1692, 2013.
Martin, M.: Cutadapt removes adapter sequences from high-throughput sequencing reads, EMBnet J, 17, https://doi.org/10.14806/ej.17.1.200, 2011.
Milkov, A. V. and Etiope, G.: Revised genetic diagrams for natural gases based on a global dataset of >20,000 samples, Org Geochem, 125, 109-120, https://doi.org/10.1016/j.orggeochem.2018.09.002, 2018.
Moore, T. R. and Dalva, M.: Methane and carbon dioxide exchange potentials of peat soils in aerobic and anaerobic laboratory incubations, Soil Biol Biochem, 29, 1157-1164, https://doi.org/10.1016/s0038-0717(97)00037-0, 1997.
Nakamura, F. M.: Microcosms and the role of active microbiota on methane cycle in soils under Forest and Pasture of Eastern Amazon, Centro de Energia Nuclear na Agricultura, Universidade de São Paulo, Piracicaba, 117 pp., https://doi.org/10.11606/T.64.2019.tde-14072021-141002, 2019.
Oertel, C., Matschullat, J., Zurba, K., Zimmermann, F., Erasmi, S., Greenhouse gas emissions from soils—A review. Geochemistry 76, 327–352. https://doi.org/10.1016/j.chemer.2016.04.002, 2016
Oremland, R. S., Whiticar, M. J., Strohmaier, F. E., and Kiene, R. P.: Bacterial ethane formation from reduced, ethylated sulfur compounds in anoxic sediments, Geochim Cosmochim Ac, 52, 1895-1904, https://doi.org/10.1016/0016-7037(88)90013-0, 1988.
Pekney, N. J., Diehl, J. R., Ruehl, D., Sams, J., Veloski, G., Patel, A., Schmidt, C., and Card, T.: Measurement of methane emissions from abandoned oil and gas wells in Hillman State Park, Pennsylvania, Carbon Management, 9, 165-175, https://doi.org/10.1080/17583004.2018.1443642, 2018.
Pfadenhauer, J. and Klötzli, F.: Restoration experiments in middle European wet terrestrial ecosystems: an overview, Vegetatio, 126, 101-115, https://doi.org/10.1007/bf00047765, 1996.
Raimi, D., Krupnick, A. J., Shah, J. S., and Thompson, A.: Decommissioning Orphaned and Abandoned Oil and Gas Wells: New Estimates and Cost Drivers, Environ Sci Technol, 55, 10224-10230, https://doi.org/10.1021/acs.est.1c02234, 2021.
Rankin, T., Strachan, I. B., and Strack, M.: Carbon dioxide and methane exchange at a post-extraction, unrestored peatland, Ecol Eng, 122, 241-251, https://doi.org/10.1016/j.ecoleng.2018.06.021, 2018.
Riddick, S. N., Mauzerall, D. L., Celia, M. A., Kang, M., and Bandilla, K.: Variability observed over time in methane emissions from abandoned oil and gas wells, Int J Greenh Gas Con, 100, https://doi.org/10.1016/j.ijggc.2020.103116, 2020.
Romanak, K., Yang, C., and Darvari, R.: Towards a Method for Leakage Quantification and Remediation Monitoring in the Near-surface at Terrestrial CO_2 Geologic Storage Sites, Enrgy Proced, 114, 3855-3862, https://doi.org/10.1016/j.egypro.2017.03.1517, 2017.
Romanak, K. D., Bennett, P. C., Yang, C., and Hovorka, S. D.: Process-based approach to CO_2 leakage detection by vadose zone gas monitoring at geologic CO_2 storage sites, Geophys Res Lett, 39, https://doi.org/10.1029/2012gl052426, 2012.
Romanak, K. D., Wolaver, B., Yang, C., Sherk, G. W., Dale, J., Dobeck, L. M., and Spangler, L. H.: Process-based soil gas leakage assessment at the Kerr Farm: Comparison of results to leakage proxies at ZERT and Mt. Etna, Int J Greenh Gas Con, 30, 42-57, https://doi.org/10.1016/j.ijggc.2014.08.008, 2014.
Samano, P. S. G., Cahill, A. G., Timmis, R., and Busch, A.: Constraining well integrity and propensity for fugitive gas migration in surficial soils at onshore decommissioned oil and gas well sites in England, Int J Greenh Gas Con, 119, https://doi.org/10.1016/j.ijggc.2022.103712, 2022.
Saunois, M., Stavert, A. R., Poulter, B., Bousquet, P., Canadell, J. G., Jackson, R. B., Raymond, P. A., Dlugokencky, E. J., Houweling, S., Patra, P. K., Ciais, P., Arora, V. K., Bastviken, D., Bergamaschi, P., Blake, D. R., Brailsford, G., Bruhwiler, L., Carlson, K. M., Carrol, M., Castaldi, S., Chandra, N., Crevoisier, C., Crill, P. M., Covey, K., Curry, C. L.,

Etiope, G., Frankenberg, C., Gedney, N., Hegglin, M. I., Höglund-Isaksson, L., Hugelius, G., Ishizawa, M., Ito, A., Janssens-Maenhout, G., Jensen, K. M., Joos, F., Kleinen, T., Krummel, P. B., Langenfelds, R. L., Laruelle, G. G., Liu, L., Machida, T., Maksyutov, S., McDonald, K. C., McNorton, J., Miller, P. A., Melton, J. R., Morino, I., Müller, J., Murguia-Flores, F., Naik, V., Niwa, Y., Noce, S., O'Doherty, S., Parker, R. J., Peng, C., Peng, S., Peters, G. P., Prigent, C., Prinn, R., Ramonet, M., Regnier, P., Riley, W. J., Rosentreter, J. A., Segers, A., Simpson, I. J., Shi, H., Smith, S. J., Steele, L. P., Thornton, B. F., Tian, H., Tohjima, Y., Tubiello, F. N., Tsuruta, A., Viovy, N., Voulgarakis, A., Weber, T. S., van Weele, M., van der Werf, G. R., Weiss, R. F., Worthy, D., Wunch, D., Yin, Y., Yoshida, Y., Zhang, W., Zhang, Z., Zhao, Y., Zheng, B., Zhu, Q., Zhu, Q., and Zhuang, Q.: The Global Methane Budget 2000–2017, Earth Syst Sci Data, 12, 1561-1623, https://doi.org/10.5194/essd-12-1561-2020, 2020.

Savage, K., Phillips, R., and Davidson, E.: High temporal frequency measurements of greenhouse gas emissions from soils, Biogeosciences, 11, 2709-2720, https://doi.org/10.5194/bg-11-2709-2014, 2014.

Schloemer, S., Oest, J., Illing, C. J., Elbracht, J., and Blumenberg, M.: Spatial distribution and temporal variation of methane, ethane and propane background levels in shallow aquifers – A case study from Lower Saxony (Germany), J Hydrol Reg Stud, 19, 57-79, https://doi.org/10.1016/j.ejrh.2018.07.002, 2018.

Schloss, P. D., Westcott, S. L., Ryabin, T., Hall, J. R., Hartmann, M., Hollister, E. B., Lesniewski, R. A., Oakley, B. B., Parks, D. H., Robinson, C. J., Sahl, J. W., Stres, B., Thallinger, G. G., Van Horn, D. J., and Weber, C. F.: Introducing mothur: open-source, platform-independent, community-supported software for describing and comparing microbial communities, Appl Environ Microbiol, 75, 7537-7541, https://doi.org/10.1128/AEM.01541-09, 2009.

Schoell, M.: The hydrogen and carbon isotopic composition of methane from natural gases of various origins, Geochim Cosmochim Ac, 44, 649-661, https://doi.org/10.1016/0016-7037(80)90155-6, 1980.

Schout, G., Griffioen, J., Hassanizadeh, S. M., Cardon de Lichtbuer, G., and Hartog, N.: Occurrence and fate of methane leakage from cut and buried abandoned gas wells in the Netherlands, Sci Total Environ, 659, 773-782, https://doi.org/10.1016/j.scitotenv.2018.12.339, 2019.

Schwen, A., Jeitler, E., and Böttcher, J.: Spatial and temporal variability of soil gas diffusivity, its scaling and relevance for soil respiration under different tillage, Geoderma, 259-260, 323-336, https://doi.org/10.1016/j.geoderma.2015.04.020, 2015.

~~Sechman, H.: Detailed analysis of gaseous components in soil gases around petroleum wells – An effective tool for evaluation of their integrity, App Geochem, 142, https://doi.org/10.1016/j.apgeochem.2022.105346, 2022.~~

~~Sikora, A., Detman, A., Chojnacka, A., and Blaszczyk, M. K.: Anaerobic Digestion: I. A Common Process Ensuring Energy Flow and the Circulation of Matter in Ecosystems. II. A Tool for the Production of Gaseous Biofuels, in: Fermentation Processes, https://doi.org/10.5772/64645, 2017.~~

Strack, M., Keith, A. M., and Xu, B.: Growing season carbon dioxide and methane exchange at a restored peatland on the Western Boreal Plain, Ecol Eng, 64, 231-239, https://doi.org/10.1016/j.ecoleng.2013.12.013, 2014.

Strack, M., Cagampan, J., Fard, G. H., Keith, A. M., Nugent, K., Rankin, T., Robinson, C., Strachan, I. B., Waddington, J. M., and Xu, B.: Controls on plot-scale growing season CO_2 and CH_4 fluxes in restored peatlands: Do they differ from unrestored and natural sites?, Mires Peat, 17, 1-18, https://doi.org/10.19189/MaP.2015.OMB.216, 2016.

Sundh, I., Nilsson, M., Granberg, G., and Svensson, B. H.: Depth distribution of microbial production and oxidation of methane in northern boreal peatlands, Microb Ecol, 27, 253-265, https://doi.org/10.1007/BF00182409, 1994.

Sundh, I., Nilsson, M., Mikkelä, C., Granberg, G., and Svensson, B. H.: Fluxes of Methane and Carbon Dioxide on peat-mining Areas in Sweden, AMBIO, 29, 499-503, https://doi.org/10.1579/0044-7447-29.8.499, 2000.

Takai, K. and Horikoshi, K.: Rapid detection and quantification of members of the archaeal community by quantitative PCR using fluorogenic probes, Appl Environ Microbiol, 66, 5066-5072, https://doi.org/10.1128/AEM.66.11.5066-5072.2000, 2000.

Turetsky, M. R., Kotowska, A., Bubier, J., Dise, N. B., Crill, P., Hornibrook, E. R., Minkkinen, K., Moore, T. R., Myers-Smith, I. H., Nykanen, H., Olefeldt, D., Rinne, J., Saarnio, S., Shurpali, N., Tuittila, E. S., Waddington, J. M., White, J. R., Wickland, K. P., and Wilmking, M.: A synthesis of methane emissions from 71 northern, temperate, and subtropical wetlands, Glob Chang Biol, 20, 2183-2197, https://doi.org/10.1111/gcb.12580, 2014.

Versantvoort, W., Guerrero-Cruz, S., Speth, D. R., Frank, J., Gambelli, L., Cremers, G., van Alen, T., Jetten, M. S. M., Kartal, B., Op den Camp, H. J. M., and Reimann, J.: Comparative Genomics of *Candidatus* Methylomirabilis Species

and Description of *Ca.* Methylomirabilis Lanthanidiphila, Front Microbiol, 9, 1672, https://doi.org/10.3389/fmicb.2018.01672, 2018.

Vielstädte, L., Karstens, J., Haeckel, M., Schmidt, M., Linke, P., Reimann, S., Liebetrau, V., McGinnis, D. F., and Wallmann, K.: Quantification of methane emissions at abandoned gas wells in the Central North Sea, Mar Pet Geol, 68, 848-860, https://doi.org/10.1016/j.marpetgeo.2015.07.030, 2015.

Vielstädte, L., Haeckel, M., Karstens, J., Linke, P., Schmidt, M., Steinle, L., and Wallmann, K.: Shallow Gas Migration along Hydrocarbon Wells-An Unconsidered, Anthropogenic Source of Biogenic Methane in the North Sea, Environ Sci Technol, 51, 10262-10268, https://doi.org/10.1021/acs.est.7b02732, 2017.

von Goerne, G., Weinlich, F. H., and May, F.: Anforderungen und Vorschläge zur Erstellung von Leitfäden und Richtlinien für eine dauerhafte und sichere Speicherung von CO2, Bundesanstalt für Geowissenschaften und Rohstoffe, 2010.

Webster, G., Newberry, C. J., Fry, J. C., and Weightman, A. J.: Assessment of bacterial community structure in the deep sub-seafloor biosphere by 16S rDNA-based techniques: a cautionary tale, J Microbiol Methods, 55, 155-164, https://doi.org/10.1016/s0167-7012(03)00140-4, 2003.

Welpelo, C., Dubbert, M., Tiemeyer, B., Voigt, C., and Piayda, A.: Effects of birch encroachment, water table and vegetation on methane emissions from peatland microforms in a rewetted bog, Sci Rep, 14, 2533, https://doi.org/10.1038/s41598-024-52349-0, 2024.

Whiticar, M. J.: The Biogeochemical Methane Cycle, in: Hydrocarbons, Oils and Lipids: Diversity, Origin, Chemistry and Fate, 1-78, https://doi.org/10.1007/978-3-319-54529-5_5-1, 2020

Whiticar, M. J.: Carbon and hydrogen isotope systematics of bacterial formation and oxidation of methane, Chem Geol, 161, 291-314, https://doi.org/10.1016/s0009-2541(99)00092-3, 1999.

Williams, J. P., Regehr, A., and Kang, M.: Methane Emissions from Abandoned Oil and Gas Wells in Canada and the United States, Environ Sci Technol, 55, 563-570, https://doi.org/10.1021/acs.est.0c04265, 2021.

Wilson, D., Farrell, C. A., Fallon, D., Moser, G., Muller, C., and Renou-Wilson, F.: Multiyear greenhouse gas balances at a rewetted temperate peatland, Glob Chang Biol, 22, 4080-4095, https://doi.org/10.1111/gcb.13325, 2016.

Wittnebel, M., Frank, S., and Tiemeyer, B.: Aktualisierte Kulisse organischer Böden in Deutschland. [dataset], https://doi.org/10.3220/DATA20230510130443-0, 2023.

Yang, S., Wen, X., and Liebner, S.: *pmoA* gene reference database (fasta-formatted sequences and taxonomy) [dataset], https://doi.org/10.5880/GFZ.5.3.2016.001, 2016.